ELSEVIER

Coordination Chemistry Reviews
219–221 (2001) 839–879

COORDINATION CHEMISTRY REVIEWS

www.elsevier.com/locate/ccr

Photoswitchable coordination compounds

Philipp Gütlich [a,*], Yann Garcia [a], Theo Woike [b]

[a] *Institut für Anorganische Chemie und Analytische Chemie, Johannes Gutenberg Universität, Staudingerweg 9, 55099 Mainz, Germany*
[b] *Institut für Kristallographie, Universität zu Köln, Zülpicherstraße 49b, 50647 Köln, Germany*

Received 16 November 2000; received in revised form 7 February 2001; accepted 26 March 2001

Dedicated to Professor A.B.P. Lever on the occasion of his 65th birthday

Contents

Abstract

Photoswitchable compounds represent an attractive class of materials in coordination chemistry. Recent progress dealing with transition metal compounds involving photo-in-

* Corresponding author. Tel.: +49-613-1392-2383; fax: +49-613-1392-2990.
E-mail address: p.guetlich@uni-mainz.de (P. Gütlich).

PII: S0010-8545(01)00381-2

duced changes of the magnetic and/or optical properties to long-lived metastable states are covered in the present review article. The basic photophysical phenomena together with representative examples such as nitroprusside derivatives, relevant spin crossover complexes, stilbenoid complexes and finally Prussian blue analogues are discussed. Some possible applications regarding energy and information storage are suggested at the end.

Keywords: Spin crossover; LIESST; Photomagnetism; Photo-isomerization; Sodium nitroprusside; Prussian blue analogues

1. Introduction

Photoreactivity is a widespread phenomenon in organic and in inorganic chemistry. A compound may change its structural and electronic properties under light irradiation. Light-induced charge separation or *cis–trans* isomerization processes under light are well-known examples. As a consequence, a phase transformation may occur, with or without hysteresis. If the light-induced new phase possesses sufficiently long lifetime and differs in optical and/or magnetic properties such that it can be detected easily by optical or magnetic means, the material bears the potential for possible technical applications in switching or display devices.

The present account deals with light-induced changes of the magnetic and/or optical properties of transition metal compounds to long-lived metastable states. Fig. 1 sketches the general situation: a complex compound with ground state spin S and orbital momentum Γ converts under light of wavelength λ, to a more or less metastable state with spin and orbital momentum S' and Γ'. The metastable state lies higher in energy and usually has weaker metal–ligand (M–L) bonds and accordingly longer bond lengths r(M–L) than the ground state, this being the consequence of an increasing population of antibonding molecular orbitals and simultaneously decreasing population of weakly π-backbonding molecular orbitals. The energy barrier between the potential wells governs the lifetime of the

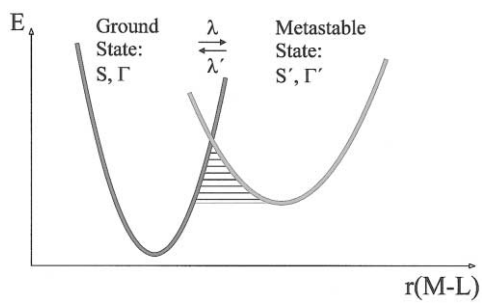

Fig. 1. Schematic representation of the potential wells for the ground state with quantum numbers S and Γ and metastable state (S' and Γ') for a transition metal compound. The switching process between these states may be provoked by irradiation with light of wavelength λ, or λ' for the reverse process.

metastable state, which in turn depends on the horizontal and vertical displacements relative to each other. Switching back from the metastable state to the ground state may be possible by using light of different wavelength λ'. The two-potential-well scheme of Fig. 1 refers to transition metal complexes with strong and intermediate field strength ligands. In weak-field complexes the potential with the longer M–L bond length would be the ground state, but light-induced switching is still possible.

There are various classes of transition metal compounds all of which show light sensitive electronic structural changes accompanied by drastic changes of their magnetic and/or optical properties. Among the best known and extensively studied systems are those exhibiting:

- metal-centered thermal spin transition, e.g. spin crossover (SC) complexes of Fe^{II};
- metal-to-ligand charge transfer, e.g. nitroprusside complexes;
- metal-to-metal charge transfer, e.g. Prussian blue analogues;
- ligand isomerization with change of spin state, e.g. stilbenoid complexes;
- valence tautomerism, e.g. catecholate complexes of Co^{II};
- open/close switching of ligands with change of spin state, e.g. diarylethene type ligands.

These classes of switchable molecular systems are currently subject to extensive research activities in many laboratories with the ultimate goal of arriving at suitable materials for technical applications such as displays, information and energy storage, and sensors [1–4]. Of utmost importance thereby is, of course, the deepest possible insight into the fundamental photophysical processes taking place locally in the individual complex molecules as the primary events as well as the short and long-range cooperative interactions, which finally are responsible for setting up hysteresis phenomena as a prerequisite for molecular bistability to occur in such materials.

The basic photophysical phenomena together with some representative transition metal compounds out of the above mentioned classes will be described in the following sections.

2. Light-induced metastable states in $Na_2[Fe(CN)_5NO]\cdot 2H_2O$ and related complexes

Hauser et al. reported in 1977 on the surprising observation that the well known sodium nitroprusside complex, $Na_2[Fe(CN)_5NO]\cdot 2H_2O$ (SNP), can be partially converted by irradiation with blue–green light to a long-lived metastable state, which they detected by Mössbauer spectroscopy as a new quadruple doublet of an Fe^{III}-LS species [5]. This was the starting point of extensive research activities on this complex compound employing a great variety of physical techniques, which by now has yielded a vast amount of information on the electronic and molecular structure, thermodynamic and kinetic properties of the light-induced metastable states. Furthermore, one has found that this kind of photophysical effect occurs not

only in the classical nitroprusside complex, but also in closely related complexes with the general composition of $X_n[ML_mNO] \cdot YH_2O$ containing the nitrosyl ligand NO. X_n are the cations or anions depending on the charge of the complex, M is the central atom (e.g. Fe, Ru, Os, Mo, Ni), L_m are the ligands (e.g. F, Cl, Br, I, CN, NH_3, NO_2, OH) and Y denotes the water content, including zero. The best analyzed system at present, however, is the complex $Na_2[Fe(CN)_5NO] \cdot 2H_2O$, in which two metastable states SI and SII can be excited by irradiation with light in the spectral range of about 350–590 nm. The completely reversible deexcitation into the ground state (GS) can be obtained by illumination in the red and near infrared spectral region of about 600–900 nm or by heating over the decay temperatures of about 150 K (SII) and 200 K (SI). Illumination with near infrared light of about 900–1200 nm partly transfers SI into SII [6]. The different spectral regions for the population and depopulation, the transfers and a potential scheme are summarized in Fig. 2.

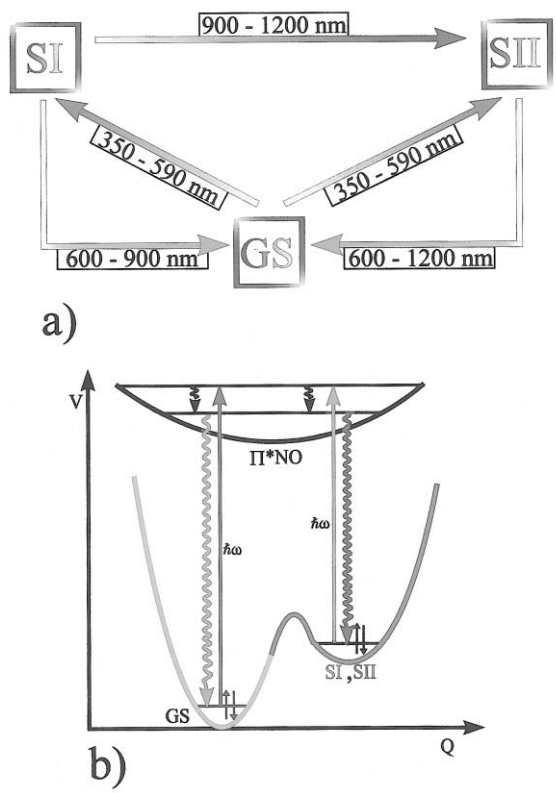

Fig. 2. (a) The spectral regions for the population and depopulation of SI and SII and the transfers between SI, SII and GS. (b) Potential scheme of the ground and metastable states with the π*(NO) orbital as the intermediate state for the relaxation into SI, SII or back into GS.

The metastable states are located in the region of the Fe–N–O bonds [7]. Of decisive importance is the energetically low lying empty π*(NO) orbital, which is positioned between the completely filled mainly Fe($3d_{xz,yz}$,$3d_{xy}$) and the empty Fe($3d_{x^2-y^2}$,$3d_z^2$) orbitals. As depicted in Fig. 2b, the population of SI and SII is a two-step-process with an intermediate metal-to-ligand charge transfer: Fe($3d_{xz,yz}$,$3d_{xy}$) → π*(NO) ⇒ SI, SII. Thereby the formally $3d^4_{xz,yz}$, $3d^2_{xy}$ diamagnetic ground state configuration [8,9] is also realized in SI and SII, however, with an energetic shift of the $3d_{xy}$ orbital and probably also of the $3d_{xz,yz}$ orbitals to higher energies of altogether about 1 eV. The lifetime of the excited π*(NO) state is in the range of 20–80 μs at 80 K, which is long enough for the rearrangement of the rest-electron density on the iron central atom. Consequently, the hyperspace is changed and the radiationless decay from the π*(NO) orbital occurs into the new potential minima of SI and SII. This excitation process is valid for each of the transition metals mentioned above. As a general conclusion, it can be stated that every excited antibonding state with sufficient lifetime is the starting point of a rearrangement of the hyperspace with possible electronic or structural consequences.

SNP crystallizes in the centrosymmetric orthorhombic space group *Pnnm* with $Z = 4$ [10–13]. As shown in Fig. 3a the central iron atom is surrounded in the first coordination sphere by five carbon atoms and one nitrogen atom. The symmetry of the fourfold axis is broken by the C–Fe–N4 angle (176.7°) and the Fe–N–O angle (175.7°). The anions lie with their quasi-fourfold axis N–C–Fe–N–O, symbolized by arrows in Fig. 3b, in antiparallel couples in the a–b mirror plane. The φ_C angle is formed by the C–Fe axis and the φ_N angle by the Fe–N axis with respect to the crystallographic a-axis. Large single crystals can be grown from saturated aqueous solution at about 315 K.

In the following sections, the basic experiments and their interpretations in order to understand the metastable states are presented. Their physical background is still an open question and is controversially discussed.

2.1. Mössbauer spectroscopy

As mentioned above, Hauser et al. discovered the metastable state SI in SNP by Mössbauer spectroscopy [5]. During the irradiation of a single crystal with the light of an Ar^+-laser (454.5–528.7 nm) and a polarization $E \| c$-axis at 80 K they detected besides the well-known quadrupole doublet of SNP a new one, showing a larger quadrupole splitting (ΔE_Q) and a more positive isomer shift (δ). The number of transferred anions from GS into SI, called population, depends on the product of incoming intensity I_L and irradiation time t and saturates at a population of about 50%, using the laser lines 454.5 or 457.9 nm. Later, it could be shown that SII has also a larger quadrupole splitting and a more positive isomer shift. The line widths of the ground state and SI are the same, but that of SII is somewhat larger [14–16]. Angle dependent Mössbauer spectra were also recorded at 80 K [15]. With this method structural as well as electronic changes can be detected.

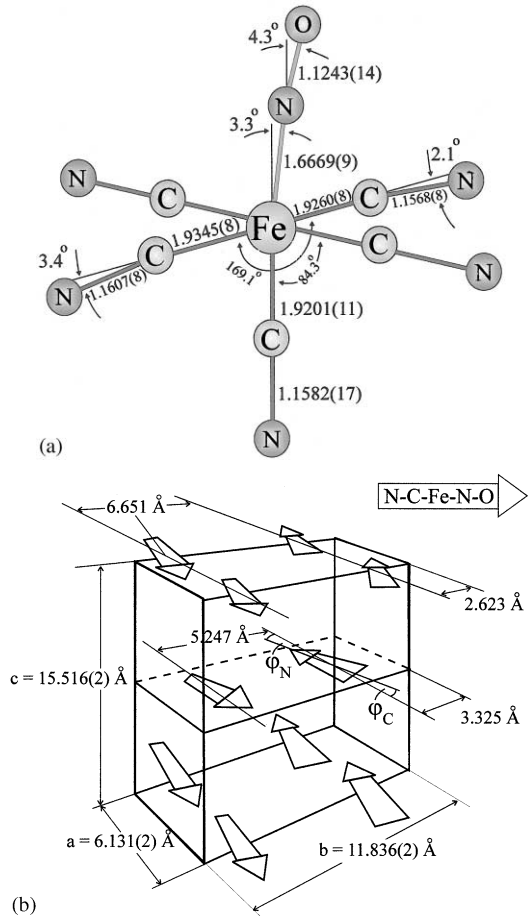

Fig. 3. (a) Structure of the $[Fe(CN)_5NO]^{2-}$ anion. (b) Schematic representation of the anions in the unit cell. The arrows indicate the direction of the N–C–Fe–N–O quasi-fourfold axis of the anion.

From the measured quadruple splitting ΔE_Q, the electric field gradient (EFG), $q = V_{zz}/e$, can be calculated using the recently calculated nuclear quadrupole moment Q [17], and the asymmetry parameter η: $\Delta E_Q = 1/2e^2Qq(1 + 1/3\eta^2)^{1/2}$ [18]. As shown in Ref. [15], the positive sign of the electric field gradient is determined by the axial symmetry of the anion, formed by the first coordination sphere of the axial carbon and nitrogen atoms C–Fe–N, so that this axial symmetry is unaffected after the excitation to the new states, and ΔE_Q is positive in all states. The orientation parameter α is given by the relation $\alpha = 1/2(\varphi_C + \varphi_N)$, which describes the composition of the direction of the EFG by the C–Fe–N bonds. Using the constant angle $\varphi_C = 37°$ in agreement with published structure data [19–21] the variation of φ_N can be determined as $\varphi_N(GS) = 33.8°$, $\varphi_N(SI) = 34.6°$ and $\varphi_N(SII) = 37.6°$. This increasing deviation from the fourfold symmetry is also seen

in the asymmetry parameter, especially in SII, in which the asymmetry of the x–y plane is about eight times larger compared to the ground state. Furthermore, the product $q\eta$ is proportional to the population of the $3d_{xz}$, $3d_{yz}$ and $4p_x$, $4p_y$ orbitals of the central iron atom. This product increases in SII by a factor of 13 with respect to GS, so that the very small degeneration of the Fe($3d_{xz,yz}$) orbitals in GS should be significantly split in SII. The more positive isomer shifts measured for the metastable states SI and SII as compared to the ground state GS reflects a lower electron density at the nucleus. This is a consequence of the electron transfer from the iron center to the π*(NO) molecular orbital, whereby after electron rearrangement at the iron center more s- than d-charge density is lost which finally results in a stronger decrease of s-electron density at the nucleus than the increase due to the weaker shielding effect of the decreased d-electron density [14]. The reason of the larger line-width (FWHM) Γ_1, Γ_2 of both Mössbauer lines in SII, which depends strongly on the temperature, is possibly produced by an oscillation of the EFG, due to the dynamic behavior of the N–O ligand. The principal axis of the mean-square displacement tensor ω, lying in the a–b plane and defined with respect to the crystallographic a-axis, rotates nearer to the a-axis, whereby the Debye–Waller factor f_b decreases and f_c increases. This change of the lattice dynamics is in good accordance with the detected shift of all elastic constants in SI and SII [22].

2.2. Raman and infrared spectroscopy

Mössbauer spectroscopy presents a first view inside the metastable states and restricts these states to be localized on the $[Fe(CN)_5NO]^{2-}$ anion. But the location, at which the significant changes occur, cannot be found by Mössbauer spectroscopy. Using vibrational spectroscopy, however, the most affected part of the anion can be detected. The most dramatic shift of the internal vibration bands of the anion occurs in the range of the Fe–N–O bonds. As shown in Table 1, all internal vibrations are shifted to lower energies.

Table 1
Internal vibrations of the $[Fe(CN)_5NO]^{2-}$ anion in GS, SI and SII

(cm^{-1})	GS	SI	SII
ν(C–N)	2174	2166	2162
ν(C–N)	2164	2156	2152
ν(C–N)	2158	2150	2146
ν(C–N)	2144	2136	2132
ν(N–O)	1950	1832	1664
δ(Fe–N–O)	668	583	597
ν(Fe–N)	658	566	546
ν(Fe–C)	414	405	–
ν(Fe–C)	410	399	–

All ν(C–N) stretching vibrations decrease by 8 cm^{-1} in SI and by 12 cm^{-1} in SII and the same is valid for the ν(Fe–C) stretching vibrations. Only two of them are tentatively assigned to GS and SI. Unfortunately, no data of SII are available in the range below 500 cm^{-1} due to the strong absorption of the crystal. But the ν(N–O) stretching vibrations are reduced by 118 cm^{-1} (SI) and 286 cm^{-1} (SII) and the ν(Fe–N) stretching vibrations decrease by 92 cm^{-1} (SI) and by 112 cm^{-1} (SII). The degenerate δ(Fe–N–O) deformation mode shifts to lower energies by 85 cm^{-1} (SI) and by 71 cm^{-1} (SII). These data are determined by the combination of Raman and infrared spectroscopy after the excitation of SI or SII as described above. They are in good agreement with published results [7,23–28]. In Ref. [28] the angle ϕ between the derivative of the transition dipole moment vector $\partial\mu/\partial Q$ and the crystallographic a-axis is determined for the ν(N–O) stretching vibration in GS, SI and SII, by angle dependent measurements. Within the error limits only a small increase of ϕ from 35° (GS) to 40° (SI) and to 42° (SII) could be found, so that the angle between the N–O ligand and the a-axis is a little bit larger in SI and SII, in accordance with the orientation parameter α of the Mössbauer results.

2.3. Differential scanning calorimetry (DSC)

One of the most interesting questions concerning these metastable states is their stability at sufficiently low temperatures. Since no luminescence could be found in the spectral range of 200–3300 nm, the whole stored energy is given up to the lattice and can be detected by DSC. The apparatus used (Mettler DSC 30, TA 3000) is equipped with two quartz windows and recalibrated by well-known phase transitions. The corresponding spectrum of the unirradiated crystal is subtracted from every measurement. As shown in Fig. 4 all thermal decays are exponential in time, analyzed by isothermal measurements, so that the excited anions are independent from each other and the thermal decay has to be described by an Arrhenius behavior. At 195 and 140 K the time derivative of the enthalpy H (heat flow) in dependence of time is detected. From the fitted exponential function, $dH/dt = dH_0/dt \exp(-t/\tau)$, we obtain the parameters $dH_0/dt = 2.43$ mW (SI), $dH_0/dt = 3.24$ mW (SII) as the starting values and $\tau = 178.5$ s (SI), $\tau = 253.0$ s (SII) as the lifetimes. From the Arrhenius plot in the temperature range 182–207 K for SI and 135–147 K for SII, we derive the activation energies E_A and frequency factors Z of both states as E_A (SI) = 0.68(3) eV, E_A (SII) = 0.53(3) eV and Z (SI) = $3(30) \times 10^{15}$ s^{-1}, Z (SII) = $2(40) \times 10^{17}$ s^{-1}. These high potential barriers are the reason for the stability.

It is a great advantage of the DSC method that the thermal decay can also be analyzed in the dynamic mode, using a constant heat velocity $q = dT/dt$. In this case the whole temperature range can be detected. In Fig. 5 the decay of SI and SII is presented for a heat velocity of $q = 5$ K min^{-1} after the population of SI and SII. The integrated peak area yields 57 kJ mol^{-1} for SI and 36.3 kJ mol^{-1} for SII. This enthalpy H_{tot} of SI is produced by a population of ca. 50% of all anions in the crystal, determined by Mössbauer spectroscopy, so that the energetic position of SI or SII is given by the relation:

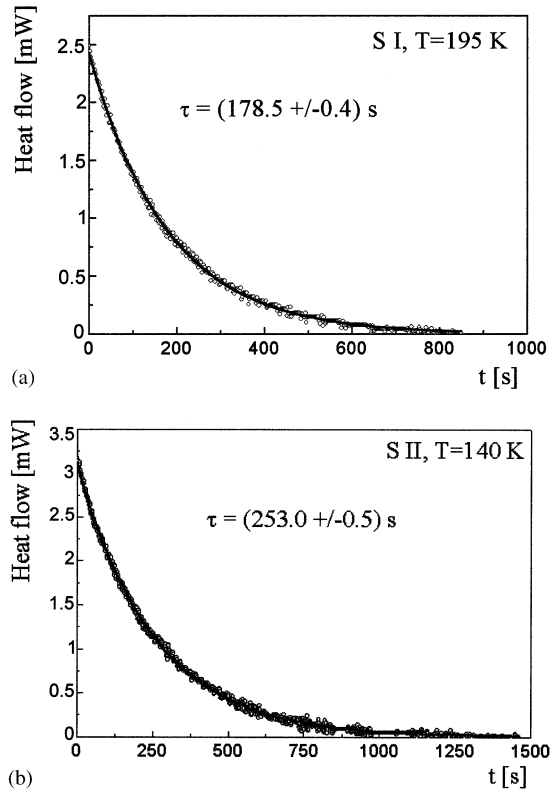

Fig. 4. Isothermal decay of: (a) SI at 195 K and (b) SII at 140 K.

$$H_{\mathrm{tot}}\,(\mathrm{kJ\ mol^{-1}}) = PE\,(\mathrm{eV}) \times 96.497 \tag{1}$$

But the whole decay cannot be fitted with only one Arrhenius ansatz, shown in Fig. 5. As evaluated in Ref. [29] two functions with the three parameters in each, viz. E_{A}, Z and H_{tot} has to be fitted:

$$\mathrm{d}H/\mathrm{d}T = H_{\mathrm{tot}} Z \exp[-\{Z/q \int \exp(-E_{\mathrm{A}}/k_B T)\mathrm{d}T + E_{\mathrm{A}}/k_B T\}] \tag{2}$$

The calculated parameter values are given in the figures.

It is possible that the thermal decay of SI and SII requires two steps or two different kinds of metastable states are excited. To clarify these questions further spectroscopic results are needed. Assuming the enthalpy H_{tot} depend linearly on the population P, the SI and SII states are estimated to lie about 1 eV above the ground state.

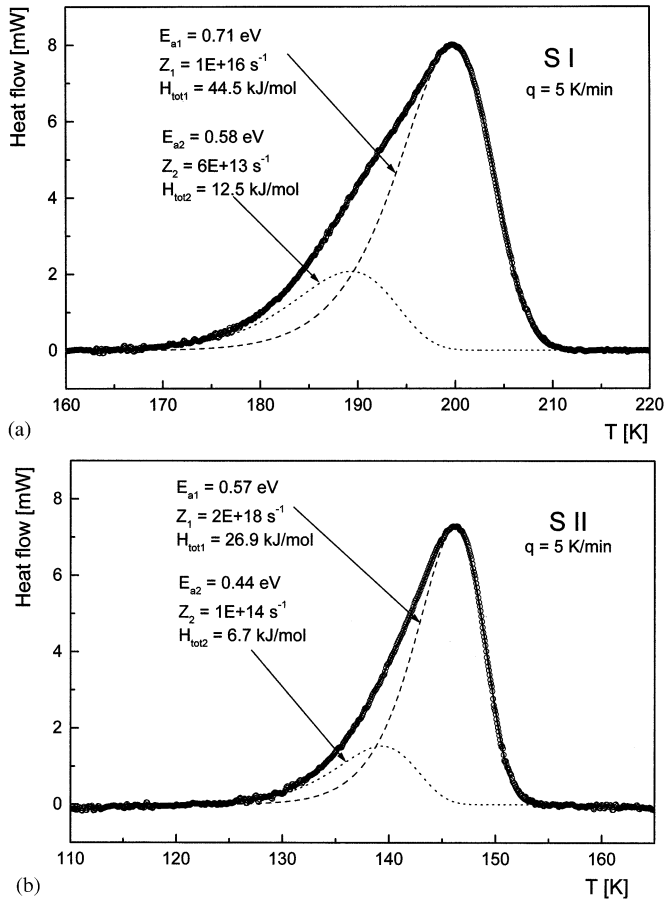

Fig. 5. Thermal decay of: (a) SI and (b) SII measured with a heat velocity of 5 K min^{-1} and fitted with the sum of two independent Arrhenius functions.

2.4. Polarized absorption spectroscopy

The drastic change of the electronic configuration after excitation to the metastable states can be detected by absorption spectroscopic measurements. The shift of the energetic positions of the highest occupied molecular orbital (HOMO) and the lowest unoccupied molecular orbital (LUMO) in SI and SII with respect to GS can be determined, keeping in mind that SI and SII lie about 1 eV above the ground state. The first experimental and theoretical determination of the energetic positions and the order of the orbitals in the ground state of the $[Fe(CN)_5NO]^{2-}$ anion was reported by Manoharan and Gray [30] and later confirmed by MSXα-calculations [31].

In Fig. 6a the ground state spectrum and the GS + SI spectra are shown after the population of 25% of the anions in SI with a light-polarization of $E \| c$-axis for the

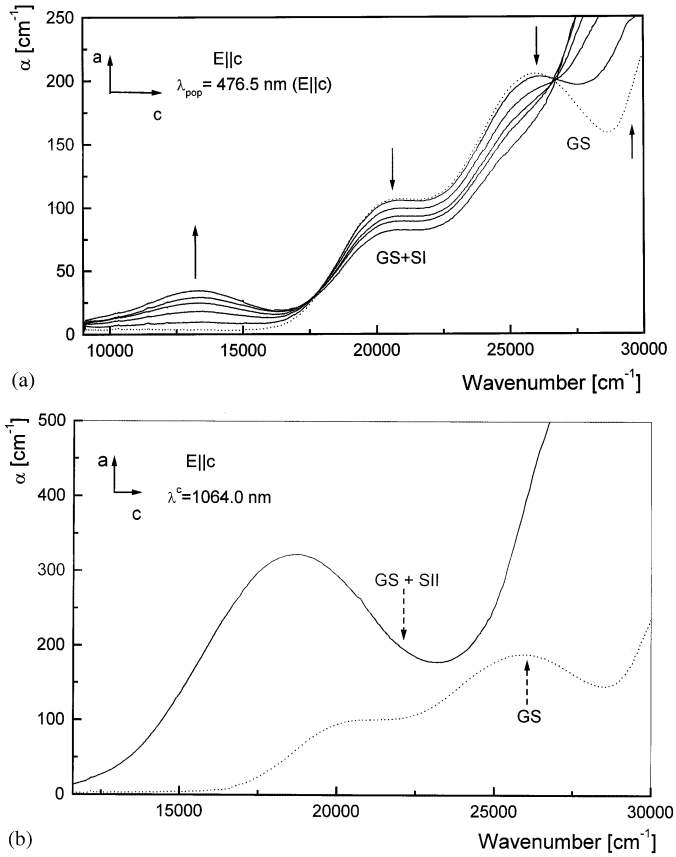

Fig. 6. (a) Absorption spectra of the ground (dotted) and metastable state SI (solid lines), irradiated and measured with $E\|c$-axis, populated with $\lambda = 476.5$ nm, and with increasing exposure time. (b) Absorption spectra of the ground and metastable state SII, irradiated and measured with $E\|c$-axis, transferred form SI into SII with $\lambda = 1064$ nm.

excitation and detection. After the population the absorption bands of GS at about 20.000 cm^{-1} (2.5 eV) and 25.000 cm^{-1} (3.1 eV) diminish and new bands in the range of about 13.000 cm^{-1} (1.6 eV) and about 29.000 cm^{-1} (3.6 eV) arise. At 18.040 and 26.700 cm^{-1}, there are two isosbestic points, from which the decreased number of the absorbing $[Fe(CN)_5NO]^{2-}$ anions in GS and the population of SI can be determined precisely, using $\alpha = N\sigma$. The cross-section σ is unaffected by the irradiation, so that the population of SI or SII is given by $P = N_{SI,SII}/N = (\alpha - \alpha_{GS})/\alpha$, where N is the total number of the anions in the unirradiated GS with the corresponding absorption coefficient α and α_{GS} is the absorption coefficient of the irradiated sample, measured in the spectral range of the decreasing GS. An independent value of α is obtained by fitting a Gaussian profile to the absorption band of GS at about 20.000 cm^{-1}, which decreases by the population of SI. For SII, the decreasing band at about 13.000 cm^{-1} can be fitted during the transfer

SI → SII. According to Refs. [30,31] and assuming 4*m* symmetry in GS, SI and SII the HOMO → LUMO transition is assigned to the $2b_2 \rightarrow 7e$ transition from the mainly Fe($3d_{xy}$) orbital into the antibonding π*(NO) orbital. In GS the following transitions are found: $2b_2 \rightarrow 7e$ (2.5 eV), 6e ($3d_{xz,yz}$) → 7e (3.1 eV), $2b_2 \rightarrow 3b_1$ ($3d_{x^2-y^2}$) (3.9 eV). In SI a clear assignment can only be given for the band at 1.6 eV as the new $2b_2 \rightarrow 7e$ transition. In Fig. 6b the ground state and GS + SII spectra are shown, whereby SII is generated by the transfer SI → SII, irradiating with $\lambda = 1064$ nm, $E \| c$-axis and an exposure of $Q = 400$ W s cm^{-2}. The transition $2b_2 \rightarrow 7e$ occurs at about 18.750 cm^{-1} (2.3 eV). In order to assign all significant transitions and especially to determine the energetic positions of the orbitals in SI or SII the absorption bands in the UV region must be known. Further, the absorption behavior along the other polarization directions ($E \| a$-, b-axis) for such an assignment and the verification of the selection rules are needed. However, irradiation with light parallel to the a- or b-axis produces very strong holographic light scattering as explained below, which is detected as a further extinction, so that no isosbestic points can be seen and especially the absorption of SII is much higher than that of GS and SI. These problems will be solved in the near future, using very thin crystals and a much higher light intensity.

2.5. Structural details and density functional calculations

The extremely long lifetime at sufficiently low temperatures opens the possibility to study the relation between the electron density, the molecular bonds and the structure of the anion in GS, SI, SII. Using thermal neutrons with energies in the range of some meV, the potential barriers are too high and possible excitations are too small to depopulate the metastable states. No significant changes were found in the structure [19,32]. The orthorhombic space group *Pnnm* of the crystal and the quasi-4*m* symmetry of the anion is conserved and the Fe–N and N–O bonds are increased by about 2%. These changes are very small in comparison with the strong rearrangement of the electronic configuration. These results were confirmed by X-ray diffraction [20]. Here the energy is much higher and it is known that a small part of the crystal water is destroyed by the radiation. Recently, in a new measurement at 50 K Carducci et al. [21] have found an increase of the lattice constants in SI and SII and they interpreted the formation of the metastable states by the structural changes of the Fe–N–O bonds in the anion as presented in Fig. 7.

The ground state has the well-known Fe–N–O configuration, in SI the N–O ligand presumably is rotated by 180° to Fe–O–N and in SII this ligand is rotated by 90°. The reason to refine the X-ray data with the Fe–O–N configuration in SI is based on the difference Fourier maps, on the charge density analysis and on the decreasing thermal parameters of the nitrogen and oxygen atoms, compared with the Fe–N–O structure. In SII they have found electron density perpendicular to the Fe–N–O axis in the region of the nitrogen atom. Therefore, the metastable states are attributed to structural changes. Unfortunately, these results could not yet be confirmed by neutron diffraction till now.

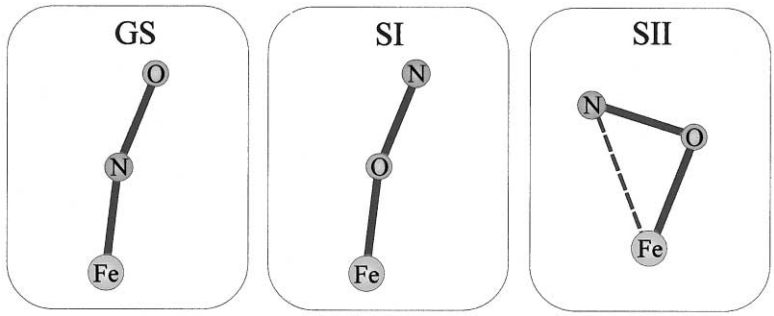

Fig. 7. The three possible structural configurations for GS, SI and SII.

However, density functional calculations for the free anion as well as for the solid have found local minima in the ground state Born–Oppenheimer surface for inverted NO (SI) and sidewards bonded NO (SII) [33]. The reaction coordinate for isomerization is identified with the Fe–N–O angle. As the local minima found in the ground state surface do not move after changing the coordinates of the Fe–N–O fragment, the excited states must be diamagnetic. The N–O, Fe–N stretching vibrations decrease and the Mössbauer quadrupole splitting increases. Further, the asymmetry parameter and isomer shift changes show the same direction as the calculated data, so that the predicted structural configurations of SI and SII [21] are supported by the density functional calculations.

2.6. Holographic measurements

The metastable states are of considerable significance for holographic information storage. Phase gratings can be written in the visible and near infrared spectral range by excitation to SI or SII [34]. The refractive index is modulated by about $\Delta n = 4 \times 10^{-2}$, which exceeds the well-known doped oxide materials, e.g. $LiNbO_3$, $LiTaO_3$, $BaTiO_3$, etc. by at least two orders of magnitude. No special dopants or defects are needed and no charge transport has to be considered. Consequently, there exists no phase shift between the written phase grating and the light modulation of the incoming writing beams [35]. The local excitation in the anions results in a local, unshifted refractive index modulation. Considering the Lorenz–Lorentz relation a modulation of the polarizability is written into the crystal, which results from the new dipole moment in the excited anions. The dipole moments calculated with DFT are 7.67 debye for the Fe–N–O ground state configuration, 6.85 debye for the N–O inversion (Fe–O–N) in SI and 5.35 debye for the 90° configuration in SII. Such a strong decrease explains the high change in the refractive index, which is important for holographic data storage. A very high data capacity can be reached, writing digital pattern in the crystal, produced by a liquid crystal. Using the bit-map of a liquid crystal with about 1 Mbit of pixels and rotating the crystal in the range from -40 to $+40°$ in steps of 0.01°, about 8000 holograms can be written (1 Gbyte) at one position. If each hologram is written

with a laser spot of 1×1 mm, a crystal with an area of about 10×10 cm is needed to store about 1Tbyte. Besides this two beam holography, gratings can also be written by only one coherent beam, which is known as light-induced holographic scattering [36]. It originates from the interference pattern of the pump and scattered waves and increases by the small signal amplification via the two-beam coupling, which occurs only in non-centrosymmetric crystals. This amplification process is bound to the presence of a polar axis. Consequently, scattered waves cannot be amplified by two-beam coupling in centrosymmetric crystals because the photorefractive response is local, so that holographic light scattering is symmetry forbidden.

However, very strong holographic light scattering could be established in centrosymmetric SNP and related compounds [37].

As shown in Fig. 8 during the population process by irradiation of the crystal with $\lambda = 514$ nm the scattered intensity increases. Fig. 8a presents the transmitted laser beam in the beginning of the irradiation and in Fig. 8b the light corona around the primary beam is shown in the saturation limit. Thousands of holographic gratings are written and the incoming light is scattered on them, producing the light corona. Rotating the crystal in any direction, this corona changes into a diffraction cone, which means that the scattered light is only seen on a ring. The Bragg condition is violated for nearly all gratings except the ones, which can be read out under this angle. This result establishes unambiguously the existence of holographic light scattering and due to the isotropic corona the centrosymmetry of SNP (*Pnnm*) in SI or SII is conserved. The assumption of a phase transition from the space group *Pnnm* into $P2_12_12$, proposed in Ref. [38] due to an assumed optical activity, can be excluded. The rotation of the incoming laser beam in a (001) cut by 90° is produced by anisotropic holographic light scattering, whereby the diffracted intensity is orthogonally polarized to the incoming beam [39].

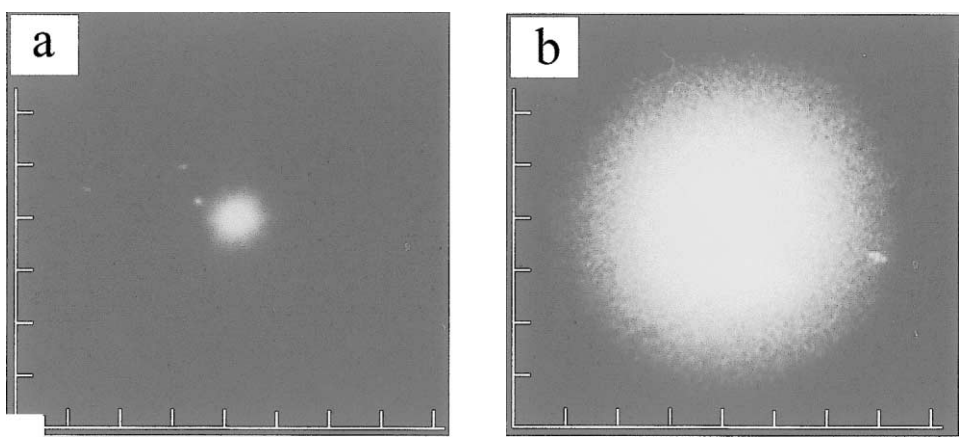

Fig. 8. (a) Transmitted laser beam in a plane behind the SNP *b*-cut crystal in the beginning of the irradiation with $E \| a$-axis, thickness $d = 250$ μm. (b) Holographic light scattering after irradiation with $\lambda = 514.5$ nm and 60 W s cm^{-2} in a *b*-cut crystal, $E \| a$-axis, thickness $d = 250$ μm.

2.7. Related complexes

The light-induced metastable states are detected in numerous compounds containing the NO ligand by changing the cation/anion, the decay temperature can be shifted in the range of about 30 K. The content of the crystal water has nearly no influence on the metastable states. Even in cooled liquids SI and SII can be generated [40]. An important increase of the decay temperature could be realized in the compounds *trans*-$[Ru(H_2O)(en)_2NO]Cl_3$ where decay sets in at about 267 K [41], $[Ru(NH_3)_5NO]Cl_3$ at about 273 K [42] and *trans*-$[Ru(Hox)(en)_2NO]Cl_2$ around 277 K [43], so that the stability of SI or SII at room temperature can be reached. A great variety of further Ru- or Os-compounds as well as the C_5H_5NiNO compound was prepared and analyzed [41–52]. In the isomorphous crystals $Na_2[M(CN)_5NO] \cdot 2H_2O$ with M = Fe, Ru, Os the decay temperature of SII is significantly shifted from about 150 K to about 230 K, in the given ordering [47,48]. It seems that the ligands are responsible for the decay temperature of SI and the central atoms determine the stability of SII. An interesting magnetic ordering effect was found by Hashimoto and coworkers [53] in the $Ni[Fe(CN)_5NO] \cdot yH_2O$ compound. The randomly aligned neighboring Ni^{II} spins are ordered after excitation to SI via two antiferromagnetically coupled spins, formed by the charge transfer transition on the NO ligand and the Fe central atom. According to the authors suggestion, these spins induce a magnetic coupling between the neighboring Ni cations forming a magnetic cluster with $S = 5$.

The photo-induced metastable states are not restricted to the NO ligand. Recently, Fomitchev et al. [54] have induced a metastable state in $[Os(NH_3)_5(N_2)](PF_6)$ with the N_2 ligand. From the structural analysis they received a 90° rotation of the N_2 ligand, which corresponds to the proposed model of SII in SNP. The SI state with 180° rotation of N–N is identical to the ground state. Related compounds with other ligands, e.g. O_2, CN, CO etc. should also show the metastable states, possibly with a short lifetime or at much lower decay temperature. It will be important to know the reaction rate and the reaction paths for possible technological applications.

Besides the information storage of up to 10 TByte a new kind of accumulator can be developed. It is possible to incorporate the anions into conducting or semi-conducting polymers [55,56], e.g. $(BEDT\text{-}TTF)_4M[Fe(CN)_5NO]_2$. The metastable state SI can be induced by light and depopulated by applying external voltage, so that the stored energy is transformed into current. In future experiments it will be important to determine the cross-section of the optical excitation and the efficiency of the current.

3. Light-induced spin state switching in iron(II) coordination compounds: LIESST and related phenomena

Iron(II) coordination compounds have never attracted much attention by spectroscopists due to the fact that, with a few exceptions (ZnS or $KMgF_3$ doped with

Fe^{II}) [57–60], iron(II) compounds do not luminesce. The more surprising was the discovery that iron(II) compounds exhibiting thermal spin transition between high-spin (HS, $^5T_2$) and low-spin (LS, $^1A_1$) states can be converted with green light from the LS ground state to a long-lived metastable HS state, and with red light back to the LS state. The first observation was made with the SC complex $[Fe(ptz)_6](BF_4)_2$ (ptz = 1-propyl-tetrazole), an iron(II) coordination compound [61,62]. The material, as single-crystal, polycrystalline or embedded in a polymer foil, converts from the LS to the HS state by irradiation with green light into the $^1A_1 \rightarrow {}^1T_{1,2}$ absorption bands, followed by two successive intersystem crossing (ISC) processes $^1T_{1,2} \rightarrow {}^3T_{1,2} \rightarrow {}^5T_2$ to populate the HS state $^5T_2$. Radiative decay $^5T_2 \rightarrow {}^1A_1$ is spin and parity forbidden, and due to the considerably larger M–L bond distance in the HS state as compared to the LS state, which builds up an energy barrier between the potential wells of the two states (see Fig. 1), the lifetime of the metastable HS state can be very long, e.g. weeks at 20 K in case of $[Fe(ptz)_6](BF_4)_2$. This phenomenon has been termed 'light-induced excited spin state trapping', abbreviated as LIESST. The mechanism is depicted in Fig. 9.

Thermal relaxation of the metastable LIESST state does not occur in a classical manner by passing over the barrier, but by non-adiabatic tunneling through the barrier, whereby the observed temperature dependence of the relaxation rate is due to thermal population of the vibronic levels of the $^5T_2$ manifold [63]. Optical

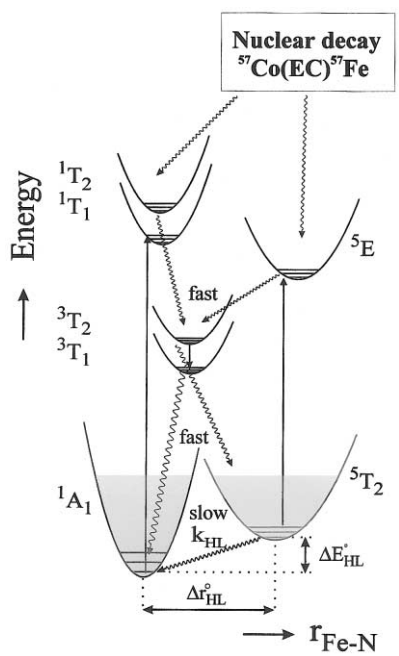

Fig. 9. Schematic illustration of LIESST and reverse LIESST of a d^6 complex in the SC range. Spin allowed d–d transitions are denoted by arrows and the radiationless relaxation processes by wavy lines (from Refs. [1a,66]).

switching back from the $^5T_2$ LIESST state to the $^1A_1$ ground state is also possible by irradiation with red light for the initial excitation $^5T_2 \rightarrow {}^5E$ followed by two ISC processes $^5E \rightarrow {}^3T_{1,2} \rightarrow {}^1A_1$. This has been termed 'reverse LIESST'. Fig. 9 shows that irradiation with red light into the spin and parity forbidden $^1A_1 \rightarrow {}^3T_1$ band should also lead to a population of the metastable $^5T_2$ state, provided the excitation wavelength is sufficiently separated from that affording the back switching of the LIESST state to the $^1A_1$ ground state [64].

Fig. 10 shows the single crystal absorption spectra of $[Fe(ptz)_6](BF_4)_2$ recorded at 20 K after irradiation at 514 nm affording the double ISC process $^1A_1 \rightarrow {}^1T_{1,2} \rightarrow {}^3T_{1,2} \rightarrow {}^5T_2$ (Fig. 10b), and at 980 nm affording the single ISC process $^1A_1 \rightarrow {}^3T_{1,2} \rightarrow {}^5T_2$ (Fig. 10d), both populating the long-lived metastable LIESST state and the reverse-LIESST effect by irradiation at 820 nm (Fig. 10c) [65].

It has been found that LIESST and reverse LIESST may be observed with all iron(II) compounds exhibiting thermal SC, a major difference, however, being the lifetime of the light-induced LIESST state at a given temperature, which depends strongly on the ligand field strength, viz. the weaker the ligand field strength, the smaller the difference ΔE^0_{HL} between the lowest vibronic levels of the HS and the LS states, the longer the lifetime of the LIESST state. The second quantity which strongly influences the lifetime of the LIESST state is the difference Δr_{HL} in the metal–ligand bond distance between HS and LS state (see Fig. 9): the larger this quantity, the longer is the lifetime of the LIESST state. The non-adiabatic multiphonon relaxation model developed by Hauser [66] based on the relaxation theory for radiationless HS → LS decay by Buhks et al. [67] describes the significance of these quantities for the lifetime of the LIESST state, whereby ΔE^0_{HL} is a measure of the vertical, and Δr^0_{HL} a measure of the horizontal displacement of the HS ($^5T_2$) and the LS ($^1A_1$) potentials relative to each other. Hauser's model [66] reproduces satisfactorily the measured temperature dependence of LIESST state relaxation rate constants: $\ln k_{HL}$ as a function of $1/T$ tends to merge into a plateau towards lower temperatures, which clearly points at quantum mechanical tunneling. At higher temperatures, $\ln k_{HL}$ increases linearly with decreasing $1/T$, but the LIESST decay is still governed by tunneling, however, between thermally populated higher vibronic levels of the HS and LS manifolds.

Hauser et al. studied the effect of an external pressure on the rate constant of HS → LS relaxation in the thermal SC system $[Zn_{1-x}Fe_x(6\text{-mepy})_3tren](PF_6)_2$ ((6-mepy)$_3$tren = tris(4-2-pyridyl-3-aza-3-butenyl)amine) [68]. They observed an eight order of magnitude increase in the low temperature tunneling rate constant between ambient pressure and 20 kbar, with an initial increase of one order of magnitude per kbar. The reason is that the external pressure increases the zero-point energy difference ΔE^0_{HL}, which corresponds to an increase in ligand field strength, which in turn shortens the lifetime of the HS state. The same physical background holds, when the LIESST state decays in a neat crystal of, e.g. $[Fe(ptz)_6](BF_4)_2$ with sigmoidal decay curves $\gamma_{LS}(t)$, the recorded LS fraction with time. $\gamma_{LS}(t)$ starts slowly, but with increasing LS concentration the decay process accelerates dramatically [63,69] due to the build-up of internal pressure as a consequence of the much smaller volume of LS as compared to HS complex molecules. Thus the intrinsic

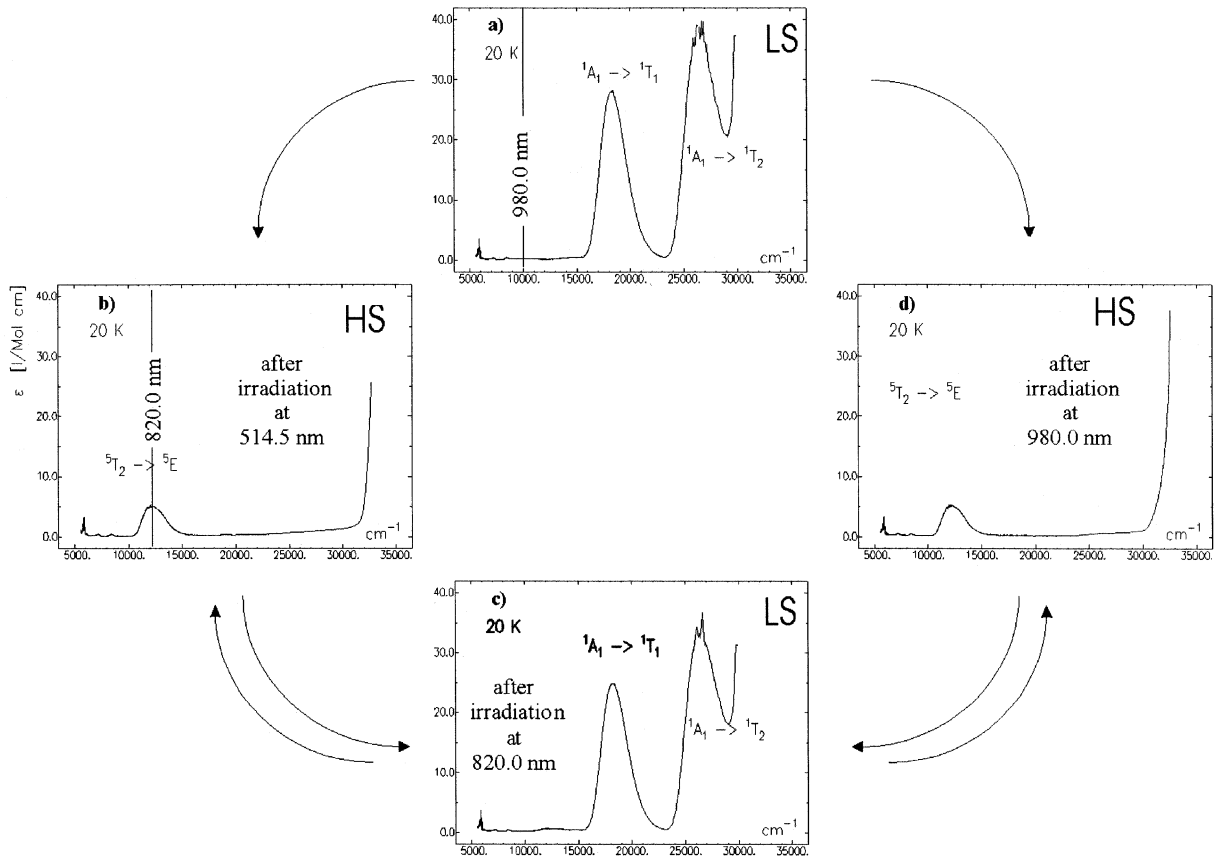

Fig. 10. Single crystal absorption spectra of $[Fe(ptz)_6](BF_4)_2$ at 20 K: (a) normal spectrum before irradiation; (b) after irradiation into the spin-allowed transition of the LS state, $^1A_1 \rightarrow {}^1T_1$, at 514.5 nm; (c) after subsequent irradiation into the maximum of the spin-allowed transition of the HS species, $^5T_2 \rightarrow {}^5E$, at 820 nm; and (d) after irradiation into the spin-forbidden transition, $^1A_1 \rightarrow {}^3T_1$, at 980 nm (from Refs. [1a,65,66]).

build-up of internal pressure increases ΔE^0_{HL} and shortens the lifetime of the LIESST state in a sigmoidal fashion. If, however, the LIESST state decays in a diluted crystal like $[Fe_{0.1}Zn_{0.9}(ptz)_6](BF_4)_2$ [69], the decay curves $\gamma_{LS}(t)$ are single-exponential. This unequivocally proves that cooperative effects are operative in a concentrated crystal, i.e. spin state changing molecules 'communicate with each other' through cooperative interactions, whereas in a diluted crystal such cooperative interactions are reduced or even vanish, like in liquid solution. This also appears to be the case for LIESST in polymer matrices [70,71] and in Langmuir–Blodgett thin films [72].

For negative values of ΔE^0_{HL}, i.e. with the HS state as the quantum mechanical ground state, no thermal spin transition is expected. In analogy to reverse LIESST it should, however, be possible to induce a HS → LS conversion by irradiation in the near infrared. For this, the potential for the ^5E state has to be above that for the $^3T_1$ state, otherwise the quantum efficiency for the first ISC step following the excitation drops to zero. Such a HS → LS conversion was first realized in the methyl substituted compound $[Fe(mtz)_6](BF_4)_2$ (mtz = 1-methyltetrazole) [73]. In this system, the complexes are distributed equally over two non-equivalent lattice sites [74]. Complexes on the one site show both a thermal spin transition as well as the light-induced processes observed in the propyl derivative. Complexes on the other site remain in the HS state down to 10 K. Irradiation in the near infrared results in a steady-state population of the LS state of around 82% for complexes on both lattice sites [75]. The LS state on the second site is a metastable state only, and at temperatures above 50 K relaxation to the HS state sets in.

The ethyl derivative $[Fe(etz)_6](BF_4)_2$ (etz = 1-ethyl-tetrazole) shows a complicated but fascinating *light-induced bistability* due to the pressure dependence of ΔE^0_{HL} [76,77]. In this system, the iron(II) complexes sit on two non-equivalent lattice sites in a ratio of 2:1. Complexes on site A show a comparatively steep thermal spin transition with a transition temperature of 105 K, those on the other site (site B) stay in the HS state down to liquid helium temperatures. Complexes on site A behave much as $[Fe(ptz)_6](BF_4)_2$ with respect to LIESST. Those on site B can be converted almost quantitatively to the LS state at 20 K by irradiating at 820 nm, into the $^5T_2 \rightarrow {}^5E$ transition of the HS species. A partial light-induced, steady-state type population of the LS state on the two sites results in an interesting relaxation behavior at temperatures below 80 K. As expected, complexes on site A always fully relax to the LS state, irrespective of the initial LS fraction, because for them ΔE^0_{HL} is always positive [77]. The relaxation behavior of B site complexes with $\Delta E^0_{HL} < 0$ depends on a critical value of the total light-induced population of the LS state. For initial values of the total LS fraction γ_{LS} of less than 0.3, complexes on site B relax to the HS state, and the system ends up with the same overall LS fraction of $\sim 2/3$, as obtained by recording a straightforward thermal transition curve. For initial values of γ_{LS} larger than 0.3, however, site B complexes, too, relax to the LS state, so that the system ends up completely in the LS state. It is clear, that as light-induced HS → LS conversion proceeds, ΔE^0_{HL} becomes positive at the critical value of $\gamma_{LS} \sim 0.3$ by virtue of the increasing internal pressure.

More recently, one has observed photophysical phenomena in iron(II) SC systems, which are related to LIESST. If a sample is continuously irradiated with green light while the temperature is raised and then lowered again, a thermal hysteresis may develop; this phenomenon has been termed 'light-induced thermal hysteresis' [78–80]. In another case one observed that an existing thermal hysteresis of an iron(II) SC compound was shifted to lower temperatures under continuous irradiation with green light, and possibly to higher temperatures with red light ('light-perturbed thermal hysteresis') [81]. Finally, 'soft X-ray induced excited spin state trapping' (SOXIESST) which uses a source of soft X-rays to initiate the $^1A_1 \rightarrow {}^5T_2$ transition [82], but the relaxation mechanism should be the same as for LIESST.

Another astonishing observation was made quite recently by ^{57}Fe Mössbauer spectroscopy on a polycrystalline sample of $[Fe_{0.02}Mn_{0.98}(terpy)_2](ClO_4)_2$ (terpy = 2,2′:6′,2″-terpyridine) [83]. In this system $[Fe(terpy)_2]^{2+}$ are accommodated statistically in the corresponding manganese host lattice and show LS behavior at room temperature. Thermal SC LS↔HS should be expected at a transition temperature $T_{1/2}$ far above room temperature. In other words, the ligand field strength and therefore ΔE^0_{HL} in this system is so large that the lifetime of the light-induced HS state is expected to be extremely short with low temperature tunneling rate constants which have been estimated on the basis of Hauser's LIESST state relaxation model to be many orders of magnitude larger than those of known thermal SC complexes (see Fig. 11). LIESST should therefore not be observable in such a strong-field complex. And yet, light-induced LS → HS conversion was in fact observed in this system with estimated decay rate constants on the order of 10^5 s at 10 K, which was still sufficiently slow for Mössbauer measurements on the ^{57}Fe enriched sample at 80 K [83]. Clearly, this unexpected observation escapes the normal LIESST mechanism. Another surprising observation of the LIESST effect was obtained recently for an Fe^{III} compound [84]. What kind of processes eventually lead to such long-lived metastable HS states remains an open question.

All complexes discussed till now are SC systems with $Fe^{II}N_6$ core. However, other SC compounds with different coordination cores such as FeP_4Cl_2 were reported to show the LIESST effect [85].

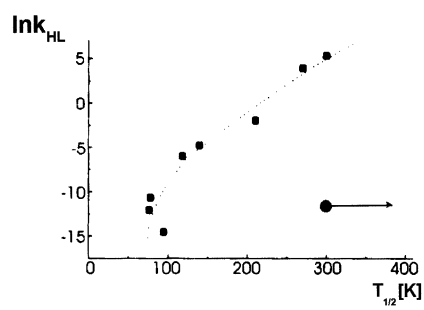

Fig. 11. Experimental low-temperature tunneling rates $\ln k^{\circ}_{HL}$ plotted against $T_{1/2}$ for some Fe^{II}-SC complexes (square) including $[Fe_{0.02}Mn_{0.98}(terpy)_2](ClO_4)_2$ (circle). The dashed line is a guide for the eyes. (from Refs. [66,84]).

4. NIESST effects

The acronym NIESST stands for 'nuclear decay-induced excited spin state trapping' observed by Mössbauer emission spectroscopy. This phenomenon is related closely to LIESST, as it makes use of the nuclear decay and its energy release as intrinsic molecular excitation source, whereas LIESST is the result of irradiation with an external visible light source. Thus the initial step of electronic excitation is different, but the final step of ligand field state relaxations has been found to be the same for both phenomena.

^{57}Fe Mössbauer emission spectroscopy (MES) is a most elegant tool for the observation of metastable ligand field states at ca. 100 ns after electron capture decay of ^{57}Co(EC)^{57}Fe in transition metal compounds [86]. In conventional ^{57}Fe Mössbauer absorption spectroscopy (MAS) one uses radioactive ^{57}Co (half-life 270 days) fused into a noble metal (Pt, Rh) as the 14.4 keV γ-ray source; the emitted single line is swept over the hyperfine transition lines of the absorber material under study by normally moving the source relative to the absorber. The recorded *Mössbauer absorption spectrum* gives information on the electronic structure (valence and magnetic state) of the ^{57}Fe atoms in the absorber material [18]. In so-called Mössbauer source experiments, one uses (in case of ^{57}Fe spectroscopy) the ^{57}Co-labeled coordination compound of special interest as the Mössbauer source, normally fixed in a cryostat for variable temperature measurements, and a single-line absorber (e.g. $K_4[Fe(CN)_6]\cdot 3H_2O$), which is mounted on a transducer and moved relative to the source. In this case, one obtains a so-called *Mössbauer emission spectrum*, which bears information on the electronic structure of the nucleogenic ^{57}Fe atom (ion) during the lifetime of the 14.4 keV nuclear state.

Already some thirty years ago, we have observed anomalous resonance lines in the Mössbauer emission spectra of ^{57}Co-labeled coordination compounds which could be assigned to metastable HS states of $^{57}Fe^{II}$ in the corresponding compounds, where Fe^{II} possesses a LS ground state at comparable temperatures [87–92]. Only with the discovery of the LIESST effect, we were able to understand the occurrence of such nuclear decay-induced metastable spin states. A few examples will be recalled in the following.

The first observation of anomalous spin states arising from the ^{57}Co(EC)^{57}Fe decay was made with phen complexes [88]. The system $[M(phen)_3](ClO_4)_2$ with $M = {}^{57}Fe_x/Co_{1-x}$, $x = 0.001$ was studied by temperature dependent Mössbauer absorption spectroscopy, and the one with $M = {}^{57}Co_x/Co_{1-x}$, $x = 0.001$ by time-integral Mössbauer emission spectroscopy (TIMES). A selection of spectra for both series is shown in Fig. 12.

The neat iron complex (M = Fe) is a typical Fe^{II}-LS compound with $^1A_1$ ground state, whereas the Co^{II} analogue is HS with $^4T_1$ ground state. If Fe^{II} is doped into the host lattice of the Co^{II} compound to only 0.1% as in the present case, the tris-phen ligand field surrounding the Fe^{II} ions is still sufficiently strong such that the Fe^{II} exhibits LS behavior at all temperatures under study; Fig. 12(a) shows a typical Fe^{II}-LS quadrupole doublet between 300 and 6 K. If, however, the Co^{II} compound is doped with radioactive $^{57}Co^{II}$ and used as a Mössbauer source against

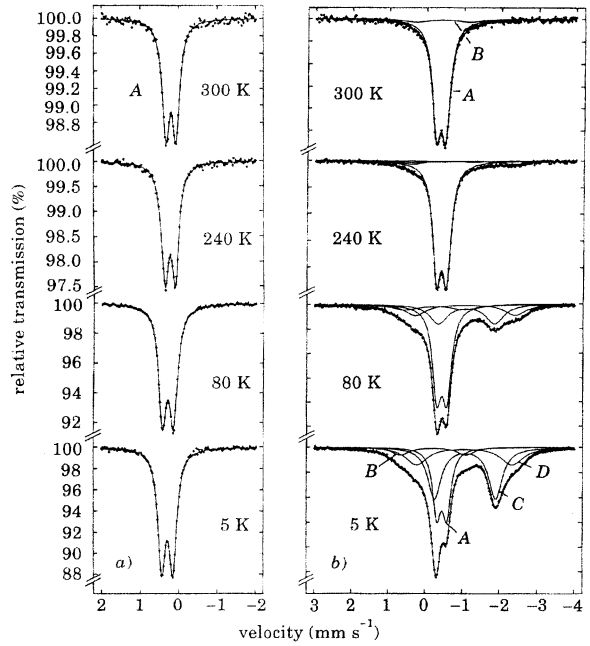

Fig. 12. (a) ^{57}Fe Mössbauer absorption spectra of $[^{57}Fe/Co(phen)_3](ClO_4)_2$ as a function of temperature vs. ^{57}Co/Rh (295 K) as source. (b) Time-integral ^{57}Fe Mössbauer emission spectra of a $[^{57}Co/Co(phen)_3](ClO_4)_2$ source as a function of temperature vs. $K_4[Fe(CN)_6]$ (295 K). Assignment: A, Fe^{II}-LS; B, Fe^{III}-LS; C, Fe^{II}-HS1; D, Fe^{II}-HS2. In (a) the source was moved relative to the absorber and in (b) the absorber was moved relative to the fixed source mounted in the crystal. For direct comparison, the sign of the velocities must be changed either (a) or (b) (from Ref. [86]).

the single-line absorber $K_4[Fe(CN)_6]$, emission spectra are obtained as shown in Fig. 12(b). Down to ca. 250 K the emission spectra are much the same as the absorption spectra and show essentially only the typical Fe^{II}-LS doublet (A) and a small fraction of Fe^{III}-LS (B), arising from the loss of a valence electron after the nuclear decay. Toward lower temperatures two typical Fe^{II}-HS resonance doublets (C and D) appear with increasing intensities at the expense of the Fe^{II}-LS doublet; the Fe^{III}-LS doublet (B), however, remains practically unchanged in intensity. According to the area fractions about half of the nucleogenic ^{57}Fe ions are 'trapped' in the metastable Fe^{II}-HS state in a strong field surroundings at ca. 10^{-7} s after the nuclear decay at 5 K.

If the ligand field strength is somewhat lowered such as in the ^{57}Co-labeled complex $[Fe(phen)_2(NCS)_2]$ as the Mössbauer source, in which thermal LS↔HS transition occurs with $T_{1/2} \approx 175$ K [93], one obtains emission spectra as shown in Fig. 13 [87].

Clearly, the dominant or even only signal at all temperatures from 296 K down to 4.2 K is the Fe^{II}-HS quadrupole doublet, even at temperatures below $T_{1/2} \approx 175$ K, where spin transition occurs to the Fe^{II}-LS ground state in the Fe^{II} complex. A

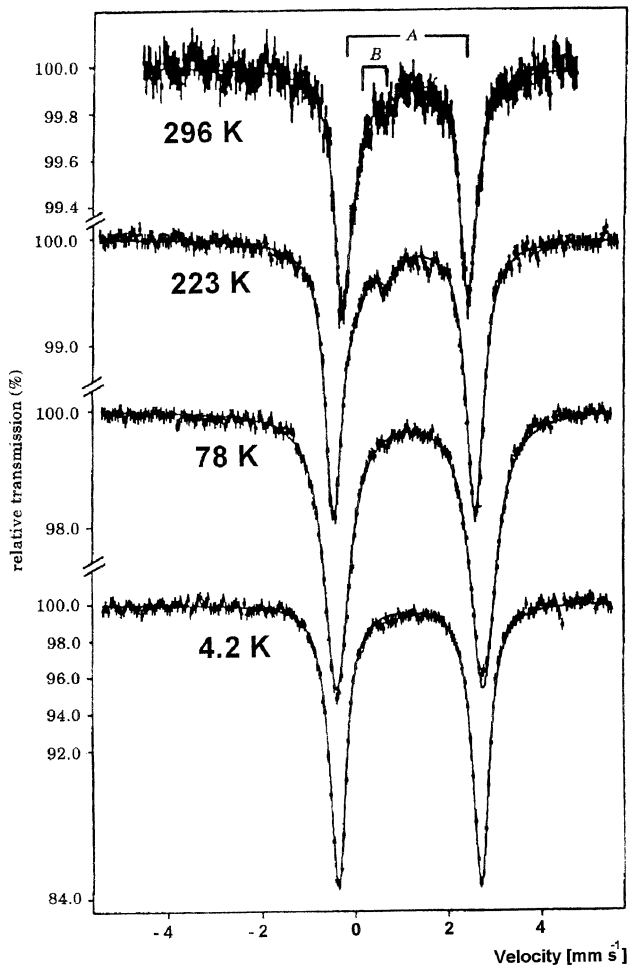

Fig. 13. ^{57}Fe Mössbauer emission spectra of a [^{57}Co/Co(phen)$_2$(NCS)$_2$] source as a function of temperature vs. $K_4[Fe(CN)_6]$ (298 K) (from Ref. [87]).

similar behavior was observed in the Mössbauer emission spectra of [^{57}Co/Co-(bipy)$_2$(NCS)$_2$] (bipy = 2,2′-bipyridyl) [87,88], [^{57}Co/Co(2-CH$_3$–phen)$_3$](ClO$_4$)$_2 \cdot 2H_2O$ [89], [^{57}Co/Co(2-CH$_2$O–phen)$_3$](ClO$_4$)$_2 \cdot 2H_2O$ [90], [^{57}Co/Co(2-pic)$_3$]Cl$_2 \cdot$ EtOH [91,92] and [^{57}Co/Co(ptz)$_6$](BF$_4$)$_2$ [94], the corresponding iron(II) of which all exhibit thermal spin crossover. Obviously, in all these Fe^{II}-SC systems metastable Fe^{II}-HS states originating from the ^{57}Co nuclear decay are 'trapped' and observed, to nearly 100% of all decay events, in the 'Mössbauer window' of ca. 100 ns after nuclear decay, whereas the ground state of Fe^{II} in the same ligand surroundings at comparable temperatures is LS ($^1A_1$). Only with the discovery of the LIESST effect (see Section 3) are we close to understand these NIESST effect observations. The mechanism for both phenomena appears to be the same except for the initial step,

which is by external light irradiation in case of LIESST, but ^{57}Co(EC)^{57}Fe decay in case of NIESST. From time-differential Mössbauer emission spectroscopy (TDMES) we know that metastable Fe^{II}-HS states exist already on the nanosecond time scale [95]. There are fast ($\ll 10^{-7}$ s) spin-allowed transitions to the $^1A_1$ ground state as well as fast ($\ll 10^{-7}$ s) ISC processes, which are favored by spin–orbit coupling as in the LIESST mechanism, populating the ^5E and then the metastable $^5T_2$ state (see Fig. 9). The branching ratio for the two decay paths (prompt decay to $^1A_1$ and population of the $^5T_2$, respectively) depends on the ligand field strength and this on ΔE^0_{HL}. The weaker the ligand field strength and therefore the smaller ΔE^0_{HL}, the higher the population of the $^5T_2$ state. This agrees with the experimental results, where the population of the $^5T_2$ state is found to be much more pronounced in the Mössbauer emission spectra of SC complexes than in a strong-field system like a tris-phen complex. This 'reduced energy gap law', i.e. the smaller the energy difference ΔE^0_{HL} between the lowest vibronic levels of the HS and LS states, the longer the lifetime of the trapped $^5T_2$ state, was demonstrated by Hauser [66] to hold for LIESST state relaxation in Fe^{II}-SC complexes.

In order to prove that the LIESST mechanism also holds for the NIESST phenomenon, at least in its final step of ligand field state relaxations, we have constructed a coincidence spectrometer for TDMES experiments for lifetime measurements between ca. 5 ns and ca. 500 ns (resolution ≈ 3.5 ns) at variable temperatures down to 4 K [96]. The TDME spectra of ^{57}Co/tris-phen source prove that the intensity of the metastable Fe^{II}-HS state increases the lower the temperature and the shorter the time interval elapsed after nuclear decay. The lifetimes of one of the HS states derived from the TDME spectra were similar to that from time-resolved optical spectroscopy on $[Fe(phen)_3]^{2+}$ embedded in a Nafion foil, e.g. 188 ns at 50 K after LIESST [97] as compared to 205 ns at 47 K for the HS state after NIESST in a polycrystalline sample [95]. The agreement is very good and is strong evidence for the validity of the proposed mechanism. Further time-resolved studies of NIESST and LIESST on the very same system, viz. single crystal of $[^{57}Co/Mn(bpy)_3](PF_6)_2$ as Mössbauer source in TDMES and the corresponding single crystal iron complex for LIESST using optical spectroscopy yielded very similar results [98].

NIESST experiments have also been carried out with $[^{57}Co/M(phen)_3](ClO_4)_2$ (M = Fe, Ni, Co, Zn) as Mössbauer sources versus $K_4[Fe(CN)_6]$ as absorber, in order to investigate the matrix influence, particularly the effect of different M^{2+} radii leading to different local pressure, on the relaxation rate of the metastable NIESST state ($^5T_2$). At a given temperature, the intensity of the nucleogenic ^{57}Fe-HS resonances was found to increase with increasing M^{2+} radius in the series M^{2+} = Fe (61 pm in LS state) < Ni (70 pm) < Co (74 pm) < Zn (75 pm) [86]. A selection of relevant emission spectra recorded at 4.2 K is shown in Fig. 14.

In view of the fact that Fe^{II}-HS has the largest M^{2+} radius of 78 pm of all metal ions involved in this study, it is expected that the host with the smallest M^{2+} ion, which is the Fe^{II}-LS with 61 pm, should have the lowest formation probability of $^{57}Fe^{II}$-HS after NIESST. This is indeed the case. The smallert the $r(M^{2+})$, the higher the local pressure, the larger ΔE^0_{HL}, the shorter the lifetime (or faster the decay) of the ^{57}Fe(HS)-HS state after NIESST.

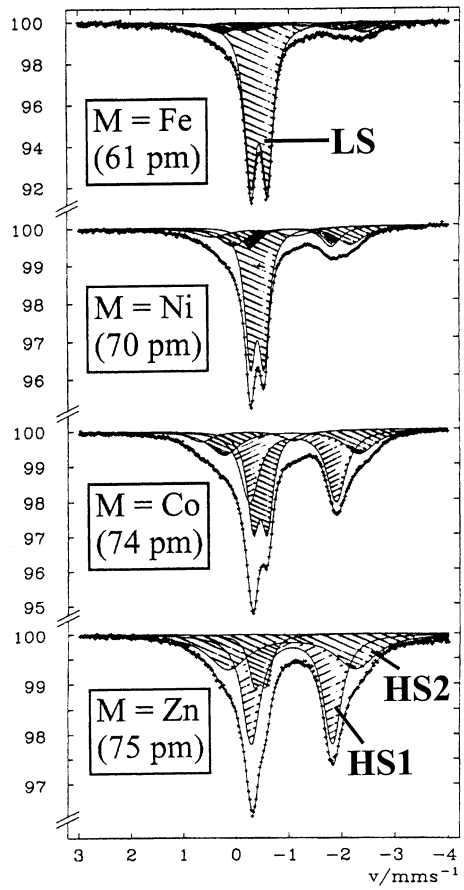

Fig. 14. ^{57}Fe Mössbauer emission spectra of $[^{57}Co/M(phen)_3](ClO_4)_2$ vs. $K_4[Fe(CN)_6]\cdot 3H_2O$ recorded at 4.2 K. The spectra show increasing intensities of the nucleogenic $^{57}Fe^{II}$-HS doublets with increasing M^{2+} radius due to decreasing local pressure (from Ref. [82]).

Similar NIESST experiments have recently been performed with $[^{57}Co/Co(bpy)_3][MCr(ox)_3]$ (M = Li, Na) and $[^{57}Co/Co(bpy)_3][MCr(ox)_3]$ (M = Li, Na) and $[^{57}Co/Co(bpy)_3][Mn_2(ox)_3]$ as Mössbauer sources. These systems possess a cubic crystal structure, where the ^{57}Co-labeled cationic complex molecules sit in a cavity of slightly different dimension [99]. The *a*-axis is the smallest (15.387 Å) in the network with Li^+ and largest in that with Mn^{II}. Thus it is expected that in the former case the relaxation of the nucleogenic $^{57}Fe^{II}$-HS state after NIESST is faster due to the somewhat higher local pressure in the former than in the latter case. This has indeed been observed: the intensity of the $^{57}Fe^{II}$-HS resonances at a given temperature is larger in the system with Na^+Cr^{3+} than in that with Li^+Cr^{3+}, but is largest in the host with $(Mn^{2+})_2$ [100]. These results are again well in accordance with the 'reduced energy gap' law.

The NIESST effect was most recently studied for the first time in a Co^{II} SC compound, viz. $[^{57}Co/Co(terpy)_2]X_2$ ($X = ClO_4^-$, Cl^-), where terpy is the tridentate ligand terpyridyl. The perchlorate derivative shows thermal spin transition, whereas the chloride derivative is still in the LS state at room temperature [101]. The former apparently possesses a weaker ligand field at the Co^{II} ion than the latter compound. In view of the 'reduced energy gap law', the perchlorate has a smaller ΔE^0_{HL} value than the chloride and should therefore yield a higher population of the Fe^{II}-HS state after NIESST than the chloride. This in fact has been observed; the emission spectra in Fig. 15, which were recorded at 100 K, show a much larger fraction of the Fe^{II}-HS doublet for the perchlorate than for the chloride [102].

NIESST studies were also performed on $[^{57}Co/Co(py)_2Ni(CN)_4]$ (py = pyridine) [103]. The corresponding 2-D cyano coordination Fe^{II}–Ni^{II} polymer is known to display an abrupt thermal spin transition $^1A_1 \leftrightarrow {}^5T_2$ around 190 K with a hysteresis of 12 K [104]. The diamagnetic Ni^{II} ions are arranged in square planar configura-

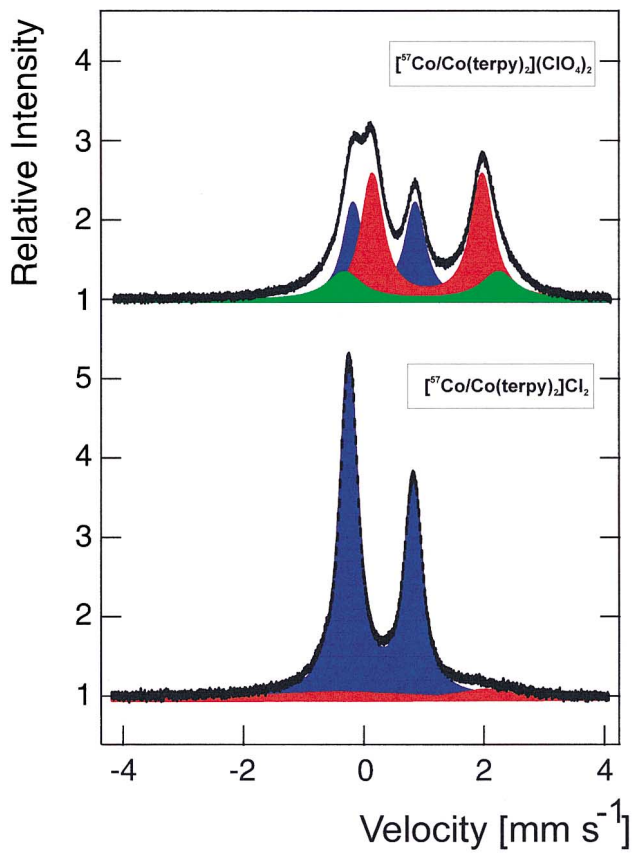

Fig. 15. Mössbauer emission spectra at 100 K for $[^{57}Co/Co(terpy)_2]A_2$ ($A = ClO_4^-$, Cl^-) (adapted from Ref. [102]).

tion whereas Fe^{II} ions have octahedral surroundings. An interesting electron transfer from Fe^{II}-HS to Fe^{III}-HS above 210 K has been observed by Mössbauer spectroscopy [103].

These examples demonstrate that the NIESST effect, which cannot be considered as a photoswitching phenomenon in the usual sense, can be used to probe local ligand field or chemical pressure differences in a very sensitive manner.

5. Stilbenoid complexes

In Section 3, we have learnt about the photoswitching of spin states of Fe^{II}-SC compounds (LIESST effect). Another way to induce a spin transition photochemically can be achieved by an indirect manner following the so-called ligand driven light-induced spin change (LD-LISC) [105–107]. This process is based on the well-known *cis–trans* photo-isomerization of stilbenoid units introduced as ligand molecules of some transition metal compounds. The 4-styrylpyridine (stpy) molecule has first been considered (Scheme 1) [106,107]. When photo-induced isomerization of the ligand proceeds as a primary step, the ligand field at the Fe^{II} ion is modified and consequently the electronic distribution and spin states too. Accordingly, in the temperature region where the isomers are present in the LS and in the HS state, the photo-isomerization of the ligand directly result in SC behavior. The first studies have been carried out on the Fe^{II} mononuclear compound $[Fe(stpy)_4(NCS)_2]$ for which the crystal structures of its *trans* and *cis* isomers have been solved [107]. The Fe^{II} ions are surrounded by six nitrogen atoms belonging to two thiocyanate groups coordinated in *trans* position and to the pyridine rings of the four stpy ligands (Fig. 16).

The *trans* form exhibits quite an abrupt spin transition at 108 K whereas the *cis* form remains permanently HS. Unfortunately, the LD-LISC effect could not be observed on this system [107]. The first observation was done actually on a related compound, $[Fe(stpy)_4(NCBPh_3)_2]$, which undergoes a sharp spin transition around ca. 190 K for the *trans* derivative, the *cis* derivative retaining the HS state down to 4.2 K (Fig. 17).

UV light irradiation of a cellulose acetate film of $[Fe(trans\text{-}stpy)_4(NCBPh_3)_2]$ around 140 K, that is in the LS area, resulted in a LS → HS conversion which was followed by absorption spectroscopy. This transformation was found to be incomplete probably due to the rigidity of the matrix at this temperature [108].

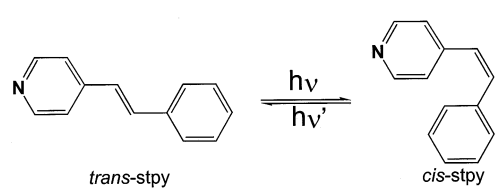

Scheme 1. *cis–trans* photo-isomerization of stpy.

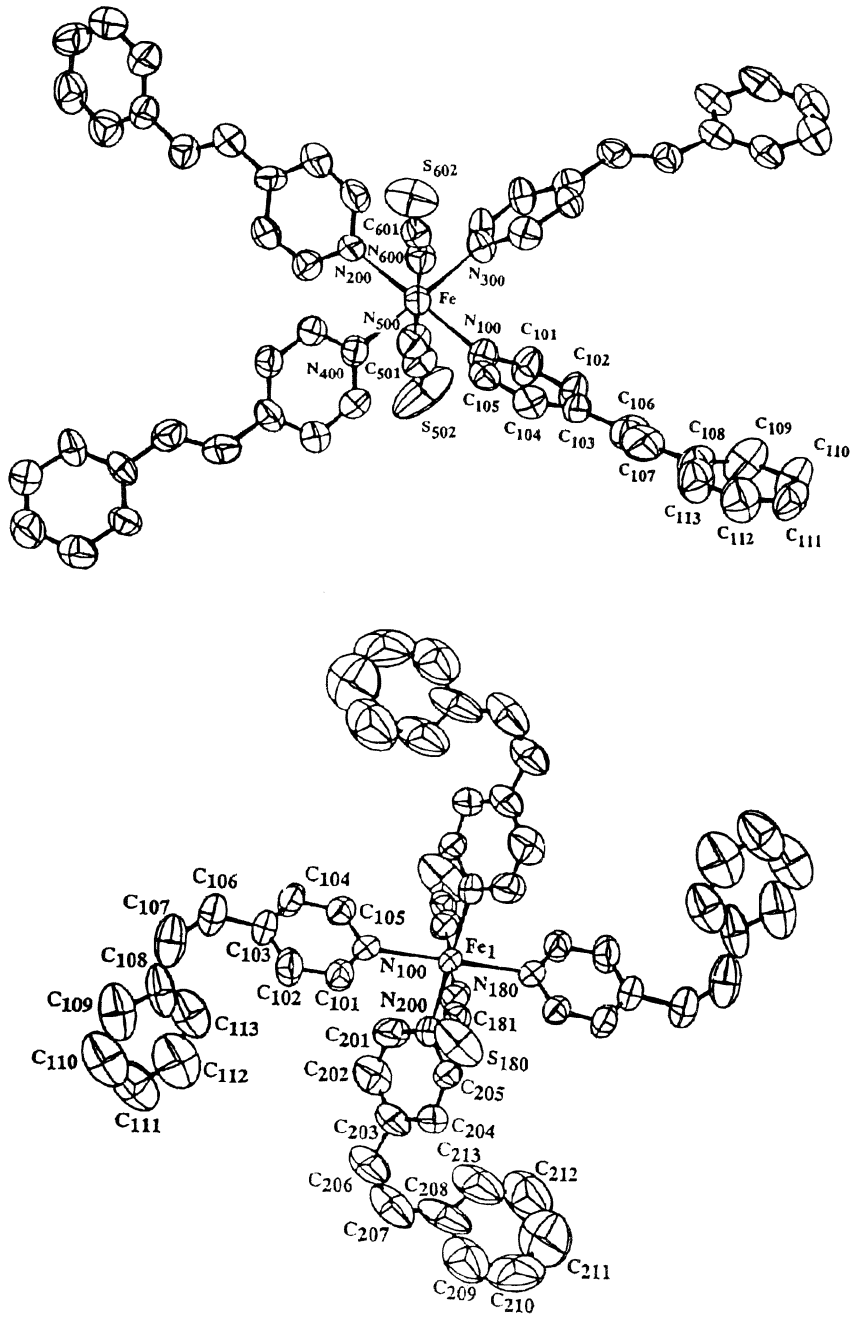

(1)

(2)

Fig. 16. Crystal structures of [Fe(*trans*-stpy)$_4$(NCS)$_2$] (**1**) and [Fe(*cis*-stpy)$_4$(NCS)$_2$] (**2**) at 293 K (from Ref. [108]).

Further efforts have been successful to increase the transition temperature of such potentially photo-isomerizable compounds [109,110]. Finally, the LD-LISC effect was observed in solution and at room temperature for $[Fe(t\text{-msbpy})_2(NCS)_2]$ (t-msbpy = 4-methyl-4′-*trans*-styryl-2,2′-bipyridine), a compound including two photosensitive ligands (Scheme 2). A strong ligand field has thus been settled by the bpy so as to shift the transition temperature of the *trans* form to higher temperatures (around ca. 264 K) [111].

One of the appealing aspects of the LD-LISC effect is that it can be extended to any transition metal ion. Therefore some Fe^{III} complexes containing photo-isomerizable ligands were investigated recently [112–115]. The salten SC complexes (salten = bis(3-salicylideneaminopropyl)amine) [115] were modified slightly such as to incorporate one photosensitive stpy molecule. $[Fe(salten)(stpy)]BPh_4 \cdot x\,Sol$ undergoes SC behavior for its two isomers, the transition temperatures of the *trans* form being the lowest. The crystal structures were also solved for both forms. The Fe^{III} ion is surrounded by three nitrogen and two oxygen atoms in *trans* position coming from the salten unit and one nitrogen atom arising from the stpy molecule in apical position (Fig. 18).

Unless photo-isomerization proceeds for the *trans* form in acetonitrile, the spin state change could not be clearly identified [114]. However, substituting stpy by a pyrole–pyridine photosensitive ligand on the same system allowed to shift the SC behavior to above room temperature and a photo-induced spin state change from HS to LS could be observed for the first time [113].

Co^{II} compounds are also subject to investigations in this context. One of them incorporating the mstpy (1-(4-methyl-phenyl)-2-(4-pyridyl)ethene) ligand has just been prepared. This complex undergoes under its *trans* form quite a gradual

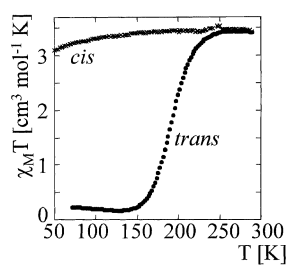

Fig. 17. Temperature dependence of $\chi_M T$ for the *trans* and *cis* forms of $[Fe(stpy)_4(NCBPh_3)_2]$ (adapted from Ref. [108]).

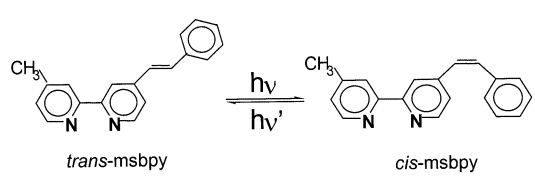

Scheme 2. *cis–trans* photo-isomerization of t-msbpy.

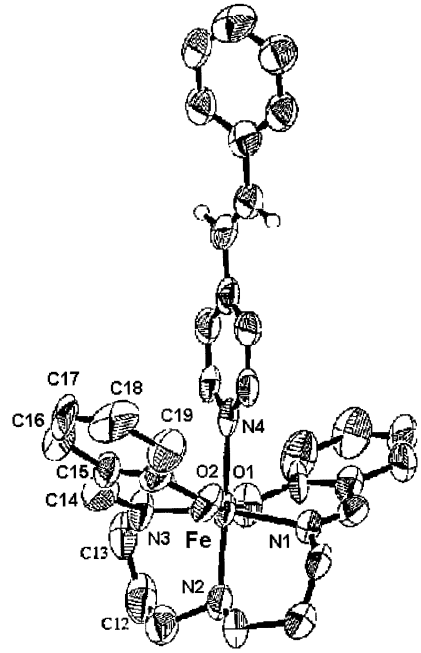

Fig. 18. Crystal structure of [Fe(salten)(*trans*-stpy)](BPh_4) · acetone · 0.5H_2O (adapted from Ref. [114]).

thermal spin conversion (LS, $S = 1/2$)↔(HS, $S = 3/2$) centered around ca. 270 K [116].

The limiting point of the LD-LISC is that it has for now only been observed in thin films or in solution, the reason being the enormous space required for the photo-isomerization of the ligand to proceed, which is not available in the solid state. This weak point regarding practical applications could be overcome by implementation of these photosensitive materials in organized media on the mesoscopic scale, such as Langmuir–Blodgett films [117].

6. Prussian blue analogues

The design of photoswitchable molecular based magnets with a high Curie temperature (T_c) represents a challenging topic in materials science both from an academic and a practical viewpoint. There has been a renewed research interest, these last five years, for one of the oldest coordination complex [118], the Prussian blue $Fe^{III}[Fe^{II}(CN)_6]_3 \cdot xH_2O$ and its derivatives [119]. These materials can show spontaneous magnetization covering a wide range of higher temperatures (from 90 to 376 K) [119–135]. Soon after the report on $V[Cr(CN)_6]_{0.86} \cdot 2.8H_2O$, the very first Prussian blue analogue having a T_c above room temperature (315 K) [123], the first photoswitchable system was communicated by Hashimoto and coworkers in 1996 [136].

$K_{0.2}Co^{II}_{1.4}[Fe^{III}(CN)_6]\cdot 6.9H_2O$ possesses a face-centered cubic structure (Fig. 19) in which Co^{II} ions are bridged to Fe^{III} ions via cyano groups, a few isolated Co^{III}–Fe^{II} diamagnetic pairs being also present in the lattice. This compound exhibits ferrimagnetic ordering below 16 K [136]. Red light irradiation at 5 K results in a spectacular enhancement of the magnetization together with a rise of T_c from 16 to 19 K (Fig. 20). This light-induced magnetization remains trapped at 5 K for several days in the dark. Switching back to the ground state is obtained by increasing the temperature to 150 K or by blue light irradiation [136].

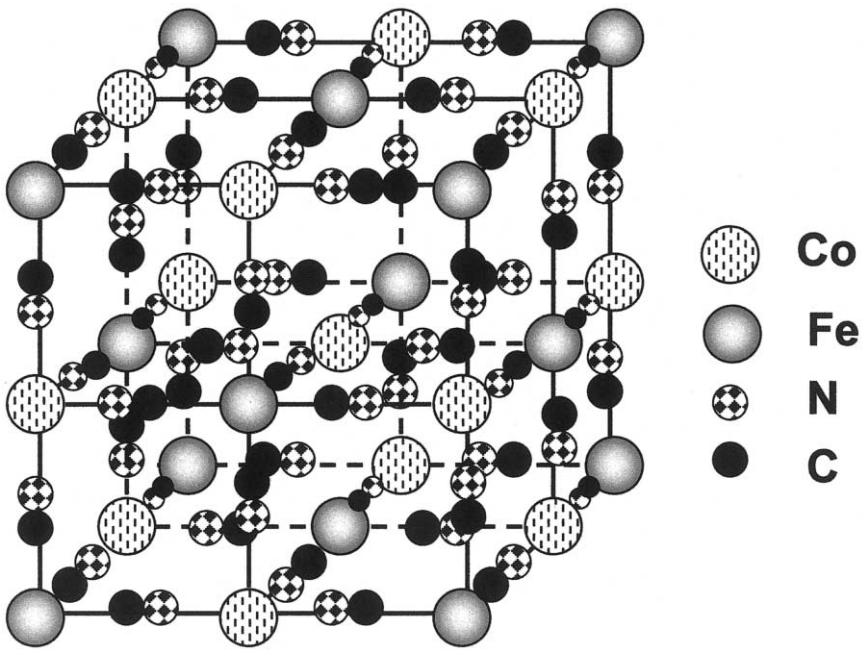

Fig. 19. Face centered cubic structure of $K_{0.2}Co_{1.4}[Fe(CN)_6]\cdot 6.9H_2O$ deduced from X-ray powder diffraction. Insertitial K^+ ions, water molecules and defects have been omitted for clarity (adapted from Ref. [136]).

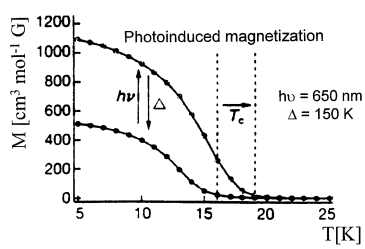

Fig. 20. Photoswitching of the magnetic properties of $K_{0.2}Co_{1.4}[Fe(CN)_6]\cdot 6.9H_2O$. The lower magnetization curve was measured before irradiation at 660 nm, and the upper one after irradiation (from Ref. [136]).

These features may be related to the presence of a charge transfer excited state at a relatively low energy above the ground state, which can be populated by visible light irradiation [137]. Actually, red light irradiation provokes an internal redox reaction induced by a photochemical electron transfer which will be detailed hereafter. Before the excitation, the Co^{III} and Fe^{II} ions are in their diamagnetic LS states ($S = 0$ for both) and there is no interaction between them. Excitation with red light induces an electron transfer from the iron to the cobalt leading to Co^{II} ions in the HS state ($S = 3/2$) and Fe^{III} ions in the LS state ($S = 1/2$), which couple antiferromagnetically leading to a ferrimagnetic behavior. This local electron transfer decreases the number of diamagnetic pairs in the solid and as a result both magnetization and T_c increase [137]. Exciting is that the reverse electron transfer is accessible by irradiation with another wavelength (Fig. 21).

From an application viewpoint, the slow switching process (a few minutes) as well as the low temperature range of the observation of the phenomenon are the weak points of this system in spite of the reversibility of the process. Anyhow, it represents the first example of fine-tuning of long-range magnetic ordering by light [137].

Photomagnetic studies on related Co–Fe cyanide materials using different alkali cations have been carried out [138–144]. One of them, $Rb_{0.66}Co_{1.25}[Fe(CN)_6] \cdot 4.3H_2O$, reveals a photo-induced long-range magnetic ordering from a paramagnetic state to a ferrimagnetic ordering ($T_c = 22$ K) when irradiated at 5 K by any wavelength in the visible region [140], due to an intense charge transfer band. The reverse process in this case is obtained only by thermal treatment. A related material which is essentially diamagnetic before irradiation (with a small amount of paramagnetic Co^{II} ions), also was found to exhibit a spectacular photo-excitation of the same type ($T_c = 21$ K) [142]. A very small effect was, however, observed on a diamagnetic compound containing cesium cations. It was therefore concluded that the presence of diamagnetic Co^{III}–Fe^{II} pairs is not a sufficient condition to observe the phenomenon; crystal defects should be present in the cubic structure so as to render the network flexible and allow the extension of

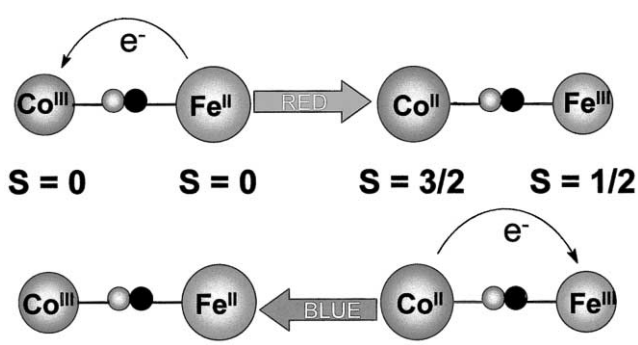

Fig. 21. Back and forth electron transfer induced by photons of different wavelengths through the cyano bridge, and the related magnetic changes (from Ref. [137]).

the light-induced electron transfer [142]. Varret et al. have focused on the shape of the thermal relaxation curves after photo-excitation. These were found to obey a self-accelerated kinetics at high temperature, whereas a weak, non-exponential behavior was observed at low temperature. These features were discussed in terms of cooperative effects in the frontal process of the photo-excitation [143].

The first thermally induced electron transfer leading to spin state changes around room temperature was discovered for $Na_{0.4}Co_{1.3}[Fe(CN)_6] \cdot 5H_2O$ [145]. Variation of the respective concentration of both cations leads to hysteresis effects also around room temperature [146]. Photochromic properties were also evidenced [147], which is appealing in terms of a possible implementation of such kind of materials in switching devices operating at the molecular level. Photomagnetic studies on these systems are currently in progress [146].

A new photomagnetic effect was discovered recently on a mixed ferro–ferrimagnet Fe^{II}–Cr^{III} cyanide derivative [148]. The temperature dependence of the magnetization of $(Fe_{0.4}Mn_{0.6})_{1.5}[Cr(CN)_6] \cdot 7.5H_2O$ shown in Fig. 22 is actually the sum of the positive magnetization of the Mn^{II} sublattice (a ferrimagnet with a T_c of 67 K) [119a,126] and two negative magnetizations of the Fe^{II} and Cr^{III} sublattices which have different temperature dependencies [149]. Upon blue light irradiation at ca. 16 K with a weak external magnetic field (10 G), the total magnetization becomes positive, revealing a magnetic pole inversion. The pole is reversed back again by thermal treatment above 80 K (Fig. 22). Thus, a photo-induced magnetic pole inversion, which can be induced repeatedly by alternate optical and thermal stimulations, has been evidenced. This discovery is important in view of the fact that the same strategy could be applied successfully to high T_c molecule based magnets, leading to the observation of a room temperature photo-induced magnetic dipole [148b].

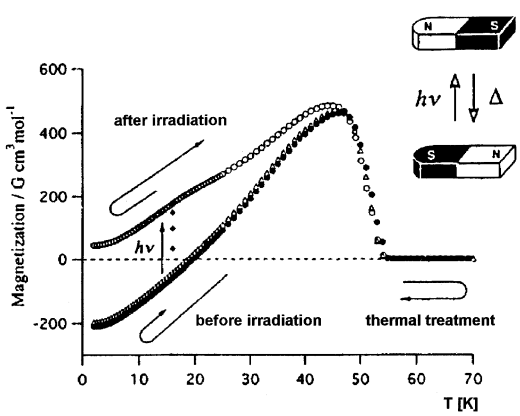

Fig. 22. Temperature dependence of the magnetization of $(Fe_{0.4}Mn_{0.6})_{1.5}[Cr(CN)_6] \cdot 7.5H_2O$ before (●) and after (○) blue light irradiation. The curves recorded after thermal treatment (△) are also shown (from Ref. [148]).

Extensive research efforts are currently carried out on Prussian blue analogues having more diffuse and high energy magnetic orbitals such as 4d or 5d so as to increase the interaction between the nearest magnetic neighbors and to obtain a fine-tuning of the magnetic properties [131,150–155]. This project actually initiated by Larionova et al. has led to the first crystal structures for 3-D analogues of Prussian blue as well as to the first magnetic phase diagrams [150]. Photomagnetic effects have also been discovered on this type of compounds [156,157]. For instance, UV light irradiation at 10 K of the 1-D bimetallic zigzag chain $[Mn^{II}_2L_2(H_2O)][Mo^{IV}(CN)_8]\cdot 5H_2O$ (L = 2,13-dimethyl-3,6,9,12,18-pentaazabicyclo[12.3.1]octadeca-1(18),2,12,14,16-pentaene, leads to a dramatic modification of the magnetic properties going from an antiferromagnetic to ferrimagnetic behavior caused by an internal photo-oxidation from diamagnetic Mo^{IV} ($S = 0$) to paramagnetic Mo^{V} ($S = 1/2$). This effect is, however, not reversible [156].

More exciting was the discovery of an electron transfer induced thermal spin transition for $Cs_{0.8}Co_{1.3}[W(CN)_8](3\text{-cyanopyridine})_{1.9}\cdot 2.1H_2O$ leading to a hysteresis of ca. 50 K around 170 K as shown in Fig. 23 [157]. At low temperatures, the compound is in its LS state and does not show any spontaneous magnetization as Co^{III} and W^{IV} are diamagnetic ($S = 0$ for both). However, visible light irradiation populates the HS state as a consequence of the electron transfer from the cobalt to the tungsten leading to paramagnetic Co^{II} ions ($S = 3/2$) and W^{V} ions ($S = 1/2$), which couple antiferromagnetically, leading to a ferrimagnetic behavior with a T_c above 30 K [157].

7. Conclusions and outlook

The photocontrol of the magnetic and optical properties remains a challenging topic in materials science in view of the possible implementation in optical switching and memory devices. Information and energy storage are also to be

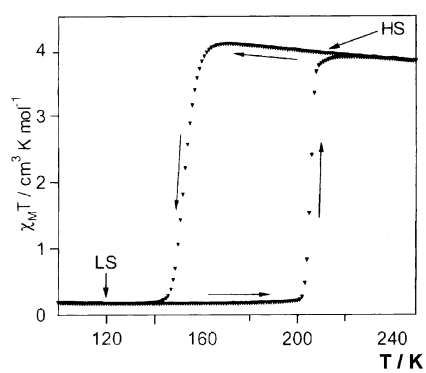

Fig. 23. $\chi_M T$ vs. T plot for $Cs_{0.8}Co_{1.3}[W(CN)_8](3\text{-cyanopyridine})_{1.9}\cdot 2.1H_2O$ in the cooling and in the heating modes (from Ref. [157]).

considered. The increasing demand for available information in science, economy and culture results in the necessity to store any desired amount of data. By the worldwide success of the internet a data quantity of some peta-byte can circulate around the world. Since these data are stored for now on available storage systems like volatile memories, hard disk, CD-ROM, magnetic tapes, etc., a lot of important and irreproducible information get lost. Meanwhile it is impossible to save all the required data; because the lifetime of all storage media in use is limited and during the re-recording further data get lost and many more new data are produced. A principal problem arises from the serial data format. The reading or writing time of, e.g. 1 TByte increases to hours working with the high speed of 10^{-9} s per bit. The more information is at our disposal the more time is needed in the serial data processing. In the field of energy storage the main difficulties arise by the conversion from one kind of energy into another one and by the losses of available battery systems, e.g. due to the discharge current. All these difficulties require a new kind of information and energy storage besides the current working systems. Long-lived metastable states produced in nitroprusside complexes and possibly other coordination compounds are very promising candidates in this regard. Due to the change of the refractive index during the excitation, information can be stored by writing volume phase holograms. No special doping is needed and a broad spectral range of excitation and deexcitation is available for the writing process. Embedding such compounds in organic conductors, the stored energy can be transferred into current by applying external voltage, in order to overcome the potential barrier, which is responsible for the metastability. Such a battery system has no losses by discharge current and can be recharged only by light. Provided, however, that the transfer rate and transfer velocity is high enough. Besides these technological applications the study of light-induced metastable states is highly relevant to chemistry, biology and materials sciences, because of the reaction path which can be induced and controlled by light.

Various examples belonging to the appealing class of photoswitchable materials have been covered in this review. There is no doubt that a sizeable number of new systems as well as new photophysical phenomena will emerge in the near future from this rapidly evolving field. The frontier of molecular based magnets is also in true progress [158–161], the addition of light effects and the combination with the above mentioned photoswitchable processes may lead to spectacular results in the near future. We can, for instance, mention a novel composite material comprising Prussian blue intercalated into photoresponsive vesicles based on azobenzene moieties, whose magnetic properties can be controlled by photo-illumination [162]. Also recently, the photosensitive NO has been introduced in a 4d Prussian blue analogue, $K_{0.9}Mn^{II}_{1.05}[Mo^{I}(CN)_5(NO)] \cdot 5H_2O \cdot 1.9MeOH$ which is ferromagnetic with a T_c of 39 K [163].

Extension of the LD-LISC to any other photochemical process like, for instance, bond forming/breaking rearrangements [164] is in principle possible. Irie et al. have reported on the reversible photoswitching of the intramolecular magnetism of two nitronyl nitroxides placed at the extremities of a photochromic diarylethene molecule [4,165]. Such spin couplers could be replaced by SC molecules yielding the

possibility to observe light-induced switching of spin states at room temperature [166]. Photo-isomerization of non-coordinated stilbenoid anions could also result in SC behavior as it is well known that non-coordinating constitutents (anions, solvent molecules) of solid coordination compounds can influence dramatically the spin state behavior of the central ion [167].

Another appealing perspective would be to investigate in depth the possible photoswitching of coordination compounds exhibiting thermal valence tautomeric interconversion [3,168,169]. To the best of our knowledge no convincing demonstration has been reported yet, but it should not be surprising if success in this regard would be communicated soon.

Acknowledgements

Financial support from the TMR Research Network 'TOSS' under EU grant No. ERB-FMRX-CT98-0199, the Fonds der Chemischen Industrie, the Materialwissenschafliches Forschungszentrum of the University of Mainz, and the Deutsche Forschungsgemeinschaft is greatly appreciated. Many thanks to M.K. Imlau, J. Schefer, B. Delley, D. Schaniel, R.A. Rupp, S. Decurtins, K. Schwarz, A. Hauser and H. Spiering for helpful discussions, measurements and DFT calculations.

References

[1] (a) P. Gütlich, A. Hauser, H. Spiering, Angew. Chem. Int. Ed. Engl. 33 (1994) 2024;
(b) P. Gütlich, Y. Garcia, H.A. Goodwin, Chem. Soc. Rev. 29 (2000) 419.
[2] P. Gütlich, Y. Garcia, Encyclopedia of Materials: Science and Technology, Pergamon/Elsevier, New York, 2001 (in press).
[3] P. Gütlich, A. Dei, Angew. Chem. Int. Ed. Engl. 36 (1997) 2734.
[4] M. Irie, Chem. Rev. 100 (2000) 1685.
[5] (a) U. Hauser, V. Oestreich, H.D. Rohrweck, Z. Physik A 280 (1977) 17;
(b) U. Hauser, V. Oestreich, H.D. Rohrweck, Z. Physik A 280 (1977) 125;
(c) U. Hauser, V. Oestreich, H.D. Rohrweck, Z. Physik A 284 (1978) 9.
[6] Th. Woike, W. Krasser, H. Zöllner, W. Kirchner, S. Haussühl, Z. Phys. D 25 (1993) 351.
[7] Th. Woike, W. Krasser, P.S. Bechthold, S. Haussühl, Phys. Rev. Lett. 53 (1984) 1767.
[8] U. Hauser, M. Klimm, L. Reder, T. Schmitz, M. Wessel, H. Zellmer, Phys. Lett. A 144 (1990) 39.
[9] C. Terrile, O.R. Nascimento, I.J. Moraes, E.E. Castellano, O.E. Piro, J.A. Guida, P.J. Aymonino, Solid State Commun. 73 (1990) 481.
[10] P.T. Manoharan, W.C. Hamilton, Inorg. Chem. 2 (1963) 1043.
[11] F. Bottomley, P.S. White, Acta Crystallogr. B 35 (1979) 2193.
[12] M.Y. Antipin, V.G. Tsirelson, M.P. Flyugge, Y.T. Struchkov, R.P. Ozerov, Sov. J. Coord. Chem. 13 (1987) 67.
[13] A. Navaza, G. Chevrier, P.M. Alzari, P.J. Aymonino, Acta Crystallogr. C 45 (1989) 839.
[14] Th. Woike, W. Kirchner, Hyung-sang Kim, S. Haussühl, V. Rusanov, V. Angelov, S. Ormandjiev, Ts. Bonchev, Hyperfine Interact. 77 (1993) 265.
[15] Th. Woike, M. Imlau, V. Angelov, J. Schefer, B. Delley, Phys. Rev. B 61 (2000) 12249.
[16] Th. Woike, unpublished results.
[17] Ph. Dufek, P. Blaha, K. Schwarz, Phys. Rev. Lett. 75 (1995) 3545.

[18] P. Gütlich, R. Link, A.X. Trautwein, Mössbauer Spectroscopy and Transition Metal Chemistry, Springer, Berlin, 1978.
[19] M. Rüdlinger, J. Schefer, G. Chevrier, N. Furer, H.U. Güdel, S. Haussühl, G. Heger, P. Schweiss, T. Vogt, Th. Woike, H. Zöllner, Z. Phys. B 83 (1991) 125.
[20] M.R. Pressprich, M.A. White, Y. Vekhter, P. Coppens, J. Am. Chem. Soc. 116 (1994) 5233.
[21] M.D. Carducci, M.R. Pressprich, P. Coppens, J. Am. Chem. Soc. 119 (1997) 2669.
[22] K. Lüghausen, H. Siegert, Th. Woike, S. Haussühl, J. Phys. Chem. Solids 56 (1995) 1291.
[23] Th. Woike, W. Krasser, P.S. Beschthold, S. Haussühl, Solid State Commun. 45 (1983) 449.
[24] W. Krasser, Th. Woike, P.S. Beschthold, S. Haussühl, J. Mol. Struct. 114 (1984) 57.
[25] W. Krasser, Th. Woike, S. Haussühl, J. Kuhl, A. Breitschwerdt, J. Raman Spectrosc. 17 (1986) 83.
[26] J.A. Guida, O.E. Piro, P.J. Aymonino, Solid State Commun. 57 (1986) 175.
[27] Y. Morioka, H. Hamaguchi, J. Phys. Chem. Solids 53 (1992) 967.
[28] J.A. Guida, P.J. Aymonino, O.E. Piro, E.E. Castellano, Spectrochim. Acta 49Z (1993) 535.
[29] Th. Woike, M. Imlau, I. Malkina, J. Thermal. Anal., submitted for publication.
[30] P.T. Manoharan, H.B. Gray, J. Am. Chem. Soc. 87 (1965) 3340.
[31] M. Braga, A.C. Pavao, J.R. Leite, Phys. Rev. B 23 (1981) 4328.
[32] J. Schefer, Th. Woike, M. Imlau, B. Delley, Eur. Phys. J. B 3 (1998) 349.
[33] B. Delley, J. Schefer, Th. Woike, J. Chem. Phys. 107 (1997) 10067.
[34] Th. Woike, M. Imlau, S. Haussühl, R.A. Rupp, R. Schieder, Phys. Rev. B 58 (1998) 8411.
[35] M. Imlau, S. Haussühl, Th. Woike, R. Schieder, V. Angelov, R.A. Rupp, K. Schwarz, Appl. Phys. B 68 (1999) 877.
[36] A. Ashkin, G.D. Boyd, J.M. Dziedzic, R.G. Smith, A.A. Ballmann, J.J. Levinstein, K. Nassau, Appl. Phys. Lett. 9 (1966) 72.
[37] M. Imlau, Th. Woike, R. Schieder, R.A. Rupp, Phys. Rev. Lett. 82 (1999) 82860.
[38] Y. Morioka, Spectrochim. Acta A 50 (1994) 1499.
[39] M. Imlau, T. Woike, R. Schieder, R.A. Rupp, Appl. Phys. Lett. 75 (1999) 16.
[40] H. Zöllner, W. Krasser, Th. Woike, S. Haussühl, Chem. Phys. Lett. 161 (1989) 497.
[41] (a) K. Ookubo, Y. Morioka, H. Tomizawa, E. Miki, J. Mol. Struct. 379 (1996) 241;
(b) M. Kawano, A. Ishikawa, Y. Morioka, H. Tomizawa, E. Miki, Y. Ohash, J. Chem. Soc. Dalton Trans. (2000) 2425.
[42] P. Coppens, D.V. Fomitchev, M.D. Carducci, K. Culp, J. Chem. Soc. Dalton Trans. (1998) 865.
[43] Y. Morioka, A. Ishikawa, H. Tomizawa, E. Miki, J. Chem. Soc. Dalton Trans (2000) 781.
[44] D.V. Fomitchev, T.R. Furlani, P. Coppens, Inorg. Chem. 37 (1998) 1519.
[45] Th. Woike, H. Zöllner, W. Krasser, S. Haussühl, Solid State Commun. 73 (1990) 149.
[46] Th. Woike, S. Haussühl, Solid State Commun. 86 (1993) 333.
[47] J.A. Guida, E.O. Piro, P.J. Aymonino, Inorg. Chem. 34 (1995) 4113.
[48] J.A. Guida, E.O. Piro, P.S. Schaiquevich, P.J. Aymonino, Solid State Commun. 101 (1997) 471.
[49] L.X. Chen, M.K. Bowman, P.A. Montana, J.R. Norris, J. Am. Chem. Soc. 115 (1993) 4373.
[50] L.X. Chen, M.K. Bowman, Z. Wang, P.A. Montana, J.R. Norris, J. Phys. Chem. 98 (1994) 9457.
[51] A. Puig-Molina, H. Müller, A.-M. Le Quéré, G. Vaughan, H. Graafsma, Å. Kvick, Z. Anorg. Allg. Chem. 626 (2000) 2379.
[52] S. Ferlay, H.W. Schmalle, G. Francese, S. Decurtins, M. Imlau, Th. Woike, Inorg. Chem., submitted for publication.
[53] (a) Z.Z. Gu, O. Sato, T. Iyoda, K. Hashimoto, A. Fujishima, J. Phys. Chem. 100 (1996) 18289;
(b) Z.Z. Gu, O. Sato, T. Iyoda, K. Hashimoto, A. Fujishima, Chem. Mater. 9 (1997) 1092.
[54] D.V. Fomitchev, K.A. Bagley, P. Coppens, J. Am. Chem. Soc. 122 (2000) 532.
[55] M. Gener, E. Canadell, S.S. Khasanov, L.V. Zorina, R.P. Shibaeva, L.A. Kushch, E.B. Yagubskii, Solid State Commun. 111 (1999) 329.
[56] (a) M. Clemente-León, E. Coronado, J.R. Galán-Mascarós, C. Giménez-Saiz, C.J. Gómez-García, J.M. Fabre, Synth. Metals 103 (1999) 2279;
(b) M. Clemente-León, E. Coronado, J.R. Galán-Mascarós, C.J. Gómez-García, E. Canadell, Inorg. Chem. 39 (2000) 5394.
[57] D. Walsh, J. Lange, Phys. Rev. B 23 (1981) 8.
[58] G.A. Ham, F.S. Slack, Phys. Rev. B 4 (1971) 777.

[59] M. Skowronski, Z. Liro, J. Lumin. 24 (1981) 253.
[60] E.E. Vogel, O. Mualin, H.J. Schulz, M. Thiede, Z. Phys. Chem. 201 (1997) 373.
[61] S. Decurtins, P. Gütlich, C.P. Köhler, H. Spiering, A. Hauser, Chem. Phys. Lett. 105 (1984) 1.
[62] S. Decurtins, P. Gütlich, K.M. Hasselbach, H. Spiering, A. Hauser, Inorg. Chem. 24 (1985) 2174.
[63] A. Hauser, Coord. Chem. Rev. 111 (1991) 275 (and references therein).
[64] A. Hauser, Chem. Phys. Lett. 124 (1986) 543.
[65] P. Gütlich, A. Hauser, H. Spiering, in: E.I. Solomon, A.B.P. Lever (Eds.), Inorganic Electronic Structure and Spectroscopy, vol. II, Wiley, New York, 1999.
[66] A. Hauser, Comments Inorg. Chem. 17 (1995) 17.
[67] E. Buhks, G. Navon, M. Bixon, J. Jortner, J. Am. Chem. Soc. 102 (1980) 2918.
[68] W. Wang, I.Y. Chan, S. Schenker, A. Hauser, J. Chem. Phys. 106 (1997) 3817.
[69] A. Hauser, P. Gütlich, H. Spiering, Inorg. Chem. 25 (1986) 4245.
[70] A. Hauser, J. Adler, P. Gütlich, Chem. Phys. Lett. 152 (1988) 468.
[71] A. Hauser, A. Vef, P. Adler, J. Chem. Phys. 95 (1991) 8710.
[72] J.-F. Letard, O. Nguyen, H. Soyer, C. Mingotaud, P. Delhaès, O. Kahn, Inorg. Chem. 38 (1999) 3020.
[73] P. Poganiuch, S. Decurtins, P. Gütlich, J. Am. Chem. Soc. 112 (1990) 3270.
[74] L. Wiehl, Acta Crystallogr. B 40 (1993) 280.
[75] R. Hinek, P. Gütlich, A. Hauser, Inorg. Chem. 33 (1994) 567.
[76] (a) R. Hinek, H. Spiering, D. Schollmeyer, P. Gütlich, A. Hauser, Chem. Eur. J. 2 (1996) 1427; (b) R. Hinek, H. Spiering, P. Gütlich, A. Hauser, Chem. Eur. J. 2 (1996) 1435.
[77] A. Hauser, J. Jeftic, H. Romstedt, R. Hinek, H. Spiering, Coord. Chem. Rev. 190–192 (1999) 471.
[78] A. Desaix, O. Roubeau, J. Jeftic, J.G. Haasnoot, K. Boukheddaden, E. Codjovi, J. Linares, M. Nogues, F. Varret, Eur. Phys. B 6 (1998) 183.
[79] J.-F. Letard, P. Guionneau, L. Rabardel, J.A.K. Howard, A.E. Goeta, D. Chasseau, O. Kahn, Inorg. Chem. 37 (1998) 4432.
[80] E. Breuning, M. Ruben, J.-M. Lehn, F. Renz, Y. Garcia, V. Ksenofontov, P. Gütlich, E. Wegelius, K. Rissanen, Angew. Chem. Int. Ed. Engl. 39 (2000) 2377.
[81] F. Renz, H. Spiering, H.A. Goodwin, P. Gütlich, Hyperfine Interact. 126 (2000) 155.
[82] D. Collison, C.D. Garner, C.M. Mc Grath, J.F. Mosselmans, M.D. Roper, J.M.W. Seddon, E. Sinn, N.A. Young, J. Chem. Soc. Dalton Trans. (1997) 4371.
[83] F. Renz, H. Oshio, V. Ksenofontov, M. Waldeck, H. Spiering, P. Gütlich, Angew. Chem. Int. Ed. Engl. 39 (2000) 3699.
[84] S. Hayami, Z.-Z. Gu, M. Shiro, Y. Einaga, A. Fujishima, O. Sato, J. Am. Chem. Soc. 122 (2000) 7126.
[85] C.C. Wu, J. Jung, P.K. Gantzel, P. Gütlich, D.N. Hendrickson, Inorg. Chem. 36 (1997) 5339.
[86] H. Sano, P. Gütlich, in: T. Matsuura (Ed.), Hot Atom Chemistry, Kodanski, Tokyo, 1984, p. 265.
[87] J. Ensling, P. Gütlich, K.M. Hasselbach, B.W. Fitzsimmons, Chem. Phys. Lett. 42 (1976) 232.
[88] J. Ensling, B.W. Fitzsimmons, P. Gütlich, Angew. Chem. 9 (1970) 637.
[89] J. Fleisch, P. Gütlich, Chem. Phys. Lett. 42 (1976) 237.
[90] J. Fleisch, P. Gütlich, Chem. Phys. Lett. 45 (1977) 29.
[91] J. Fleisch, P. Gütlich, H. Köppen, Radiochem. Radioanalyt. Lett. 42 (1980) 279.
[92] P. Gütlich, H. Köppen, J. Phys. (Paris) 41 (1980) 311.
[93] W.A. Baker, H.M. Bobonich, Inorg. Chem. 3 (1964) 1184.
[94] C. Hennen, Master's Thesis, University of Mainz, 1986.
[95] R. Grimm, P. Gütlich, E. Kankeleit, R. Link, J. Chem. Phys. 67 (1977) 5491.
[96] R. Albrecht, M. Alflen, P. Gütlich, Zs. Kajcsos, R. Schulze, H. Spiering, F. Tuczek, Nucl. Instrum. Methods A 257 (1987) 209.
[97] A. Hauser, Chem. Phys. Lett. 173 (1990) 507.
[98] S. Deisenroth, A. Hauser, H. Spiering, P. Gütlich, Hyperfine Interact. 93 (1994) 1573.
[99] R. Sieber, S. Decurtins, H. Stoeckli-Evans, C. Wilson, D. Yufit, J.A.K. Howard, S.C. Capelli, A. Hauser, Chem. Eur. J. 6 (2000) 361.
[100] V. Chameko, PhD Thesis, University of Mainz, 2001.
[101] S. Kremer, W. Henke, D. Reinen, Inorg. Chem. 21 (1982) 3013.

[102] H. Oshio, H. Spiering, V. Ksenofontov, F. Renz, P. Gütlich, Inorg. Chem. 40 (2001) 1143.
[103] T. Sato, F. Ambe, T. Kitazawa, H. Sano, M. Takeda, Chem. Lett. (1997) 1287.
[104] T. Kitazawa, Y. Gomi, M. Takahashi, M. Takeda, M. Enomoto, A. Miyazaki, T. Enoki, J. Mater. Chem. 6 (1996) 119.
[105] J. Zarembowitch, C. Roux, M.L. Boillot, R. Claude, J.-P. Itie, A. Polian, M. Bolte, Mol. Cryst. Liq. Cryst. 34 (1993) 247.
[106] C. Roux, J. Zarembowitch, B. Gallois, M. Bolte, New J. Chem. 16 (1992) 671.
[107] C. Roux, J. Zarembowitch, B. Gallois, T. Granier, R. Claude, Inorg. Chem. 33 (1994) 2273.
[108] M.L. Boillot, C. Roux, J.-P. Audière, A. Dausse, J. Zarembowitch, Inorg. Chem. 35 (1996) 3975.
[109] H. Soyer, M.L. Boillot, New J. Chem. 21 (1997) 889.
[110] M.L. Boillot, A. Sour, P. Delhaes, C. Mingotaud, H. Soyer, Coord. Chem. Rev. 192 (1999) 47.
[111] M.L. Boillot, S. Chantraine, J. Zarembowitch, J.-Y. Lallemand, J. Prunet, New J. Chem. (1999) 179.
[112] (a) S. Hayami, K. Inoue, Y. Maeda, Chem. Phys. Lett. 10 (1998) 987;
(b) S. Hayami, K. Inoue, Y. Maeda, Mol. Cryst. Liq. Cryst. 334 (1999) 1285.
[113] A. Sour, M.L. Boillot, E. Rivière, P. Lesot, Eur. J. Inorg. Chem. (1999) 2117.
[114] S. Hirose, S. Hayami, Y. Maeda, Bull. Chem. Soc. Jpn. 73 (2000) 2059.
[115] (a) N. Matsumoto, S. Ohta, C. Yoshimura, A. Ohyoshi, S. Kohata, H. Okawa, Y. Maeda, J. Chem. Soc. Dalton Trans. (1985) 2575;
(b) A. Ohyoshi, J. Honbo, N. Matsumoto, S. Ohta, S. Sakamoto, Bull. Chem. Soc. Jpn. 59 (1986) 1611;
(c) S. Ohta, C. Yoshimura, N. Matsumoto, H. Okawa, A. Ohyoshi, Bull. Chem. Soc. Jpn. 59 (1986) 155;
(d) Y. Maeda, M. Suzuki, S. Hirose, S. Hayami, T. Oniki, S. Sugihara, Bull. Chem. Soc. Jpn. 71 (1998) 2837.
[116] F. Tuna, L. Patron, E. Rivière, M.L. Boillot, Polyhedron 19 (2000) 1643.
[117] (a) H. Soyer, C. Mingotaud, M.L. Boillot, P. Delhaès, Thin Solid Films 435 (1998) 327;
(b) H. Soyer, C. Mingotaud, M.L. Boillot, P. Delhaès, Langmuir 14 (1998) 5890.
[118] M.B. Robin, P. Day, Adv. Inorg. Chem. Radiochem. 10 (1967) 248.
[119] (a) M. Verdaguer, T. Mallah, V. Gadet, I. Castro, C. Hélary, S. Thiébaut, P. Veillet, Conf. Coord. Chem. 14 (1993) 19;
(b) M. Verdaguer, A. Bleuzen, C. Train, R. Garde, F.F. de Biani, C. Desplanches, Philos. Trans. R. Soc. London A 357 (1999) 2959;
(c) M. Verdaguer, A. Bleuzen, V. Marvaud, J. Vaisserman, M. Seuleiman, C. Desplanches, A. Scuiller, C. Train, R. Garde, G. Gelly, C. Lomenech, I. Rosenman, P. Veillet, C. Cartier, F. Villain, Coord. Chem. Rev. 190–192 (1999) 1023.
[120] (a) W.D. Greibler, D. Babel, Z. Naturforsh Teil B 87 (1982) 832;
(b) D. Babel, Comments Inorg. Chem. 5 (1986) 285.
[121] V. Gadet, T. Mallah, I. Castro, M. Verdaguer, J. Am. Chem. Soc. 114 (1992) 832.
[122] (a) T. Mallah, S. Thiébaut, M. Verdaguer, P. Veillet, Science 262 (1993) 1554;
(b) T. Mallah, S. Ferlay, C. Auberger, C. Helary, F. Lhermite, R. Ouahes, J. Vaissermann, M. Verdaguer, P. Veillet, Mol. Cryst. Liq. Cryst. 273 (1995) 141.
[123] S. Ferlay, T. Mallah, R. Ouahes, P. Veillet, M. Verdaguer, Nature 378 (1995) 701.
[124] (a) W.R. Entley, G.S. Girolami, Science 268 (1995) 397;
(b) W.R. Entley, C.R. Treadway, G.S. Girolami, Mol. Cryst. Liq. Cryst. 273 (1995) 153.
[125] O. Sato, T. Iyoda, A. Fujishima, K. Hashimoto, Science 271 (1996) 49.
[126] S. Okhoshi, O. Sato, T. Iyoda, A. Fujishima, K. Hashimoto, Inorg. Chem. 36 (1997) 268.
[127] O. Sato, Z.Z. Gu, H. Etoh, J. Ichiyanagi, T. Iyoda, A. Fujishima, K. Hashimoto, Chem. Lett. 1 (1997) 37.
[128] S.M. Holmes, G.S. Girolami, Mol. Cryst. Liq. Cryst. 305 (1997) 279.
[129] (a) W.E. Buschmann, S.C. Paulson, C.M. Wynn, M. Girtu, A.J. Epstein, H.S. White, J.S. Miller, Adv. Mater. 9 (1997) 645;
(b) W.E. Buschmann, S.C. Paulson, C.M. Wynn, M. Girtu, A.J. Epstein, H.S. White, J.S. Miller, Chem. Mater. 10 (1998) 1386.

[130] E. Dujardin, S. Ferlay, X. Phan, C. Desplanches, C. Cartier, P. Sainctavit, F. Baudelet, E. Dartyge, P. Veillet, M. Verdaguer, J. Am. Chem. Soc. 120 (1998) 11347.
[131] R. Garde, C. Desplanches, A. Bleuzen, P. Veillet, M. Verdaguer, Mol. Cryst. Liq. Cryst. 334 (1999) 587.
[132] S. Ferlay, T. Mallah, R. Ouahès, P. Veillet, M. Verdaguer, Inorg. Chem. 38 (1999) 229.
[133] S.M. Holmes, G.S. Girolami, J. Am. Chem. Soc. 121 (1999) 5593.
[134] Ø. Hatlevik, W.E. Buschmann, J. Zhang, J.L. Manson, J.S. Miller, Adv. Mater 11 (1999) 914.
[135] S. Ohkoshi, M. Mizuno, G. Hung, K. Hashimoto, J. Phys. Chem. B. 104 (2000) 9365.
[136] O. Sato, T. Iyoda, A. Fujishima, K. Hashimoto, Science 272 (1996) 704.
[137] M. Verdaguer, Science 272 (1996) 698.
[138] O. Sato, Y. Einaga, T. Iyoda, A. Fujishima, K. Hashimoto, J. Electrochem. Soc. 144 (1997) L11.
[139] Y. Einaga, S. Ohkoshi, O. Sato, A. Fujishima, K. Hashimoto, Chem. Lett. 7 (1998) 585.
[140] O. Sato, Y. Einaga, A. Fujishima, K. Hashimoto, Inorg. Chem. 38 (1999) 4405.
[141] T. Yokoyama, M. Kiguchi, T. Ohta, O. Sato, Y. Einaga, K. Hashimoto, Phys. Rev. B 60 (1999) 9340.
[142] (a) A. Bleuzen, C. Lomenech, A. Dolbecq, F. Villain, A. Goujon, O. Roubeau, M. Nogues, F. Varret, F. Baudelet, E. Dartyge, C. Giorgetti, J.-J. Gallet, C. Cartier, M. Verdaguer, Mol. Cryst. Liq. Cryst. 335 (1999) 253;
(b) A. Bleuzen, C. Lomenech, V. Escax, F. Villain, F. Varret, C.C.D. Moulin, M. Verdaguer, J. Am. Chem. Soc. 122 (2000) 6648;
(c) C. Cartier, F. Villain, A. Bleuzen, M.-A. Arrio, P. Sainctavit, C. Lomenech, V. Escax, F. Baudelet, E. Dartyge, J.-J. Gallet, M. Verdaguer, J. Am. Chem. Soc. 122 (2000) 6653.
[143] (a) F. Varret, H. Constant-Machado, J.L. Dormann, A. Goujon, J. Jeftic, M. Noguès, A. Bousseksou, S. Klokishner, A. Dolbecq, M. Verdaguer, Hyperfine Interact. 113 (1998) 37;
(b) A. Goujon, O. Roubeau, F. Varret, A. Dolbecq, A. Bleuzen, M. Verdaguer, Eur. Phys. J. B 14 (2000) 115.
[144] (a) D.A. Pejakovic, J.L. Manson, J.S. Miller, A.J. Epstein, J. Appl. Phys. 87 (2000) 6028;
(b) D.A. Pejakovic, J.L. Manson, J.S. Miller, A.J. Epstein, Phys. Rev. Lett. 85 (2000) 1994.
[145] O. Sato, Y. Einaga, A. Fujishima, K. Hashimoto, J. Phys. Chem. B 101 (1997) 3903.
[146] N. Shimamoto, S. Ohkoshi, O. Sato, K. Hashimoto, Mol. Cryst. Liq. Cryst. 344 (2000) 95.
[147] N. Shimamoto, S. Okhoshi, O. Sato, K. Hashimoto, Mol. Cryst. Liq. Cryst. 344 (2000) 95.
[148] (a) S. Ohkoshi, S. Yorozu, O. Sato, T. Iyoda, A. Fujishima, K. Hashimoto, Appl. Phys. Lett. 70 (1997) 1040;
(b) S. Ohkoshi, K. Hashimoto, J. Am. Chem. Soc. 121 (1999) 10591.
[149] S. Ohkoshi, Y. Einaga, A. Fujishima, K. Hashimoto, J. Electroanal. Chem. 473 (1999) 245.
[150] (a) J. Larionova, J. Sanchiz, S. Golhen, L. Ouahab, O. Kahn, Chem. Commun. 9 (1998) 953;
(b) J. Larionova, R. Clerac, J. Sanchiz, O. Kahn, S. Golhen, L. Ouahab, J. Am. Chem. Soc. 120 (1998) 13088;
(c) J. Larionova, O. Kahn, S. Gohlen, L. Ouahab, R. Clerac, J. Am. Chem. Soc. 121 (1999) 3349;
(d) J. Larionova, O. Kahn, S. Golhen, L. Ouahab, R. Clerac, Inorg. Chem. 38 (1999) 3621;
(e) J. Larionova, O. Kahn, J. Bartolome, R. Burriel, M. Castro, V. Ksenofontov, P. Gütlich, Chem. Mater. 11 (1999) 3400;
(f) J. Larionova, O. Kahn, S. Golhen, L. Ouahab, R. Clerac, J. Bartolome, R. Burriel, Mol. Cryst. Liq. Cryst. 334 (1999) 651;
(g) O. Kahn, J. Larionova, L. Ouahab, Chem. Commun. (1999) 945.
[151] J. Larionova, M. Gross, M. Pilkington, H. Andres, H. Stoeckli-Evans, H.U. Gudel, S. Decurtins, Angew. Chem. Int. Ed. Engl. 39 (2000) 1605.
[152] N. Machida, S. Ohkoshi, Z.J. Zhong, K. Hashimoto, Chem. Lett. (1999) 907.
[153] A.K. Sra, M. Andruh, O. Kahn, S. Golhen, L. Ouahab, J.V. Yakhmi, Angew. Chem. Int. Ed. Engl. 38 (1999) 2606.
[154] Z.J. Zhong, H. Seino, Y. Mizobe, M. Hidai, A. Fujishima, S. Ohkishi, K. Hashimoto, J. Am. Chem. Soc. 122 (2000) 2952.
[155] Z.J. Zhong, H. Seino, Y. Mizobe, M. Hidai, M. Verdaguer, S. Ohkoshi, K. Hashimoto, Inorg. Chem. 39 (2000) 5095.

[156] G. Rombaut, S. Golhen, L. Ouahab, C. Mathonière, O. Kahn, J. Chem. Soc. Dalton Trans. (2000) 3609.
[157] K. Hashimoto, Z.J. Zhong, S. Ohkoshi, submitted for publication.
[158] O. Kahn, Molecular Magnetism, VCH, Weinheim, 1993.
[159] M.M. Turnbull, T. Sugimoto, L.K. Thompson (Eds.), Molecule-Based Magnetic Materials. In: ACS Symposiim Series, vol. 644, American Chemical Society, Washington, DC, 1996.
[160] J.S. Miller, Inorg. Chem. 39 (2000) 4392.
[161] O. Kahn, Acc. Chem. Res. 33 (2000) 647.
[162] Y. Einaga, O. Sato, T. Iyoda, A. Fujishima, K. Hashimoto, J. Am. Chem. Soc. 121 (1999) 3745.
[163] N. Machida, S. Ohkoshi, Z.J. Zhong, K. Hashimoto, Chem. Lett. (1999) 907.
[164] L.B. Feringa, W.F. Jager, B. Delange, Tetrahedron 49 (1993) 8267.
[165] (a) K. Matsuda, M. Irie, Chem. Lett. (2000) 16;
(b) K. Matsuda, M. Irie, J. Am. Chem. Soc. 122 (2000) 7195;
(c) K. Matsuda, M. Irie, J. Am. Chem. Soc. 122 (2000) 8309.
[166] Y. Garcia, V. Ksenofontov, R. Lapouyade, P. Gütlich, Ger. Patent No. 100 39 903.7, 2001.
[167] Y. Garcia, PhD Thesis, University of Bordeaux I, 1999.
[168] O.S. Jung, D.H. Jo, Y.A. Lee, B.J. Conklin, C.G. Pierpont, Inorg. Chem. 36 (1997) 19.
[169] O.S. Jung, D.H. Jo, Y.A. Lee, Y.S. Sohn, C.G. Pierpont, Inorg. Chem. 37 (1998) 5875.